SUPPORTING INFORMATION

A range-wide postglacial history of Swiss Stone pine based on molecular markers and palaeoecological evidence

Felix Gugerli, Sabine Brodbeck, Bertalan Lendvay, Benjamin Dauphin, Francesca Bagnoli, William O. van der Knaap, Willy Tinner, Maria Höhn, Giovanni G. Vendramin, César Morales-Molino, Christoph Schwörer

Appendix 1 Information on sampling locations, lab procedures and genetic diversity of *Pinus cembra* populations from the European Alps and the Carpathians, and scenarios tested in demographic simulations.

TABLE S1.1 Sampling locations of *Pinus cembra* with geographical information. Sample numbers and measures of population genetic diversity are given for both nuclear and chloroplast microsatellite markers (simple-sequence repeats, n/cpSSRs).

				Coordinates (WGS84)		nSSRs			cpSSRs		
Range[1]	Country[2]	Code[2]	Population	Lat [°N]	Long [°E]	n	A_R	H_E	n	H	A_p
A	CH	CH01	Mürtschenalp	47.06331	9.16299	16	2.075	0.499	16	0.767	
A	CH	CH02	Neuenalp	47.17239	9.34640	16	2.121	0.529	16	0.642	
A	CH	CH03	Saflischtal	46.35504	8.11840	16	2.042	0.551	16	0.350	
A	CH	CH04	Kreuzboden	46.13763	7.95940	16	2.041	0.486	16	0.608	
A	CH	CH05	Forêt de Derbellec	46.25377	7.60046	16	2.068	0.512	16	0.450	
A	CH	CH06	Siviez	46.12703	7.32625	16	2.068	0.564	16	0.533	
A	CH	CH07	Col du Pillon	46.32938	7.08306	16	2.007	0.491	16	0.750	
A	CH	CH08	Forêt du Lapé	46.57040	7.20740	16	1.950	0.463	16	0.342	
A	CH	CH09	Rautialp	47.06733	9.00157	16	1.967	0.527	16	0.758	
A	CH	CH10	Flumserberge	47.07208	9.21131	16	2.133	0.517	16	0.342	
A	CH	CH11	Letziwald	46.46863	9.51580	16	2.158	0.537	16	0.675	
A	CH	CH12	Sardonaalp	46.92467	9.29354	16	1.936	0.556	16	0.000	
A	CH	CH13	Stazerwald	46.48736	9.87011	16	2.173	0.544	16	0.800	
A	CH	CH14	God Baselgia	46.70583	10.10686	16	2.187	0.551	16	0.808	2
A	CH	CH15	Tamangur	46.67867	10.36182	16	2.193	0.544	16	0.842	1
A	CH	CH16	Alp Sadra	46.60235	10.35350	16	2.023	0.481	16	0.875	
A	CH	CH17	Seeberg	46.67752	7.38468	16	2.060	0.508	16	0.425	
A	CH	CH18	Sagiwald	46.43986	7.64257	16	2.031	0.532	16	0.342	
A	CH	CH19	Arvengarten	46.58961	7.97150	16	2.111	0.585	16	0.342	
A	CH	CH20	Val d'Arpette	46.02252	7.07093	16	2.033	0.526	16	0.533	
A	CH	CH22	Gulmen	47.22029	9.37534	16	2.038	0.542	16	0.600	
A	CH	CH23	Darlux	46.62643	9.77351	16	2.099	0.528	16	0.667	
A	CH	CH24	God Murter	46.64726	10.01337	16	2.145	0.535	16	0.492	
A	CH	CH25	Saoseo	46.40209	10.12629	16	2.181	0.538	16	0.867	
A	CH	CH26	Lago da Cavloc	46.38361	9.70708	16	2.121	0.527	16	0.683	
A	CH	CH27	Zervreila	46.57479	9.11754	16	2.089	0.511	16	0.667	
A	CH	CH28	Lago Ritom	46.53440	8.68659	16	2.175	0.584	16	0.342	
A	CH	CH29	Riederalp	46.38830	8.01961	16	2.141	0.535	16	0.533	
A	CH	CH30	Hundsalp	46.74005	8.50902	16	1.868	0.464	16	0.817	
A	CH	CH31	Riffelalp	46.00468	7.74887	16	2.099	0.565	16	0.525	
A	CH	CH32	Sex carro	46.15798	7.07739	16	2.022	0.534	16	0.350	
A	CH	CH33	Rochers des Rayes	46.53109	7.20163	16	1.993	0.521	16	0.342	
A	CH	CH34	Val Cristallina	46.62063	8.84360	16	2.173	0.550	16	0.692	
A	CH	CH35	Alpe di Sfii	46.26066	8.48857	16	2.180	0.572	16	0.617	
A	CH	CH36	Val Masauna	46.94065	10.35628	16	2.164	0.540	16	0.800	1

A	CH	CH37	Stillberg	46.77824	9.87038	16	2.095	0.567	16	0.808	
A	CH	CH38	Alpe Arena	46.22955	8.52722	20	1.884	0.520	20	0.490	
A	CH	CH39	Selva secca	46.53909	8.82857	16	2.192	0.564	16	0.617	
A	CH	CH40	Geretal	46.53578	8.38440	16	2.036	0.552	16	0.525	
A	CH	CH41	Murgtal	47.04190	9.17215	16	2.076	0.569	16	0.608	
A	CH	CH42	Bachalp	46.34591	7.68926	16	2.097	0.578	16	0.125	
A	CH	CH43	Oberi Meiggu	46.35927	7.73721	16	1.971	0.510	16	0.575	
A	CH	CH44	Mattwald	46.32854	7.89726	16	2.087	0.524	16	0.517	
A	CH	CH45	Nufenen	46.50541	8.34689	18	2.168	0.560	18	0.307	
A	CH	CH46	Fafleralp	46.44196	7.85250	16	2.080	0.563	16	0.525	
A	CH	CH47	Nanztal	46.28595	7.97981	16	2.184	0.549	16	0.533	
A	CH	CH48	Arvenegg	46.77162	8.34549	24	2.173	0.590	24	0.797	
A	CH	CH49	In Miseren	46.73008	8.41698	24	2.128	0.576	24	0.696	
A	CH	CH50	Hubel	46.72584	8.35596	24	2.195	0.602	24	0.438	
A	CH	CH51	Arvennollen	46.67820	8.28456	24	2.122	0.580	24	0.815	
A	CH	CH52	Meder	46.56665	8.29597	24	2.111	0.523	24	0.641	
A	CH	CH53	Untersteinberg	46.50770	7.88439	24	2.077	0.556	24	0.373	
A	CH	CH54	I de Chiste	46.47548	7.67759	24	2.135	0.523	24	0.873	
A	CH	CH55	Hohberg	46.40190	7.42691	24	2.065	0.560	24	0.623	
A	CH	CH56	Schafsattel	46.53579	7.43096	24	1.975	0.524	24	0.420	
A	CH	CH57	Karblatti	46.36689	7.26873	24	2.099	0.580	24	0.797	
A	AT	AU58	Turracherhöhe	46.91750	13.88667	19	2.140	0.572	19	0.551	1
A	AT	AU59	Scheibelsee	47.44056	14.43583	19	2.139	0.608	19	0.901	
A	AT	AU60	Obergurgl	46.86219	11.01541	17	2.365	0.557	17	0.918	
A	AT	AU61a	Tockneralm	47.20422	13.94406	25	2.101	0.612	25	0.875	1
A	IT	IT62	Grubbergalm	46.97556	11.55056	20	2.242	0.587	19	0.927	
A	IT	IT63	Aleve ALE	44.61667	7.06667	25	2.170	0.506	25	0.866	
A	IT	IT64	Alpe Stavello FOR	46.35000	8.45000	25	1.975	0.548	25	0.817	1
A	IT	IT65	Bormio soil 1	46.44367	10.42125	25	2.143	0.578	25	0.657	
A	IT	IT66	GranBosco SAL	45.06667	6.91667	25	2.167	0.504	25	0.670	
A	IT	IT67	Lago Nero BOU	44.93333	6.81667	25	2.081	0.521	25	0.757	
A	IT	IT68	Manghen N 3	46.17498	11.44023	25	2.155	0.534	25	0.767	1
A	IT	IT69	Manghen S 3	46.17251	11.44264	24	2.188	0.510	24	0.900	
A	IT	IT70	Passo Oclini soil 1	46.35446	11.45490	25	2.140	0.553	25	0.859	
A	IT	IT71	Passo Oclini soil 2	46.34365	11.45238	25	2.083	0.516	25	0.887	
A	IT	IT72	Passo Sella N 3	46.50633	11.77593	25	2.107	0.542	25	0.893	
A	IT	IT73	Passo Sella S 3	46.51168	11.75094	25	2.083	0.520	25	0.877	
A	IT	IT74	Passo Tre Croci	46.56014	12.19635	25	2.138	0.549	25	0.760	1
A	IT	IT75	Saucheres SAU	45.03333	6.96667	25	2.208	0.525	25	0.913	
A	IT	IT76	Val Forni SO PICE	46.42095	10.56073	24	2.134	0.556	24	0.790	
A	IT	IT77	Val Mare soil 2	46.41513	10.68468	25	2.147	0.486	25	0.750	
A	IT	IT78	Valdieri VAL	44.16667	7.26667	25	2.060	0.573	25	0.777	

A	DE	DE79	Reiteralm	47.62548	12.79339	25	2.121	0.536	25	0.793	
A	DE	DE80	Schachen[3]	47.42600	11.12700	25	2.156	0.618	25	0.713	
A	DE	DE81	Kuehalm	47.54700	11.22900	25	2.167	0.455	26	0.866	
A	AT	AU82	Gottschallalm	47.25590	13.52829	25	1.940	0.553	25	0.689	
A	AT	AU83	St. Anton am Arlberg	47.11389	10.25000	25	2.244	0.553	25	0.800	
A	AT	AU84	Mittereggwald Kappl	47.04944	10.38528	25	2.078	0.500	25	0.687	
A	DE	DE85	Miesing Soinalm	47.64500	11.97000	31	2.094	0.594	31	0.687	
A	AT	AU86	Gappenfelder Notländ	47.44444	10.52583	25	2.156	0.498	25	0.731	
A	AT	AU87	Gottesacker	47.36422	10.12726	19	2.057	0.595	19	0.830	1
A	FR	FR88	Ayes	44.80345	6.66188	24	2.200	0.545	24	0.760	
A	FR	FR89	Boréon	44.11887	7.32874	24	2.189	0.551	24	0.808	
A	AT	AU90	Radurschtal Tscheyalpe	46.90905	10.59333	29	2.197	0.552	29	0.779	
A	FR	FR91	Val Claree	45.07231	6.51431	25	2.209	0.540	25	0.773	
A	FR	FR92	Vesubie, Fenetredela Madone	44.07708	7.35713	20	2.049	0.568	20	0.803	
A	AT	AU93	Donnersbach	47.41794	14.15047	25	2.199	0.563	25	0.721	
A	AT	AU94	Gastein Grau Kogel	47.10678	13.16707	24	2.270	0.637	24	0.850	1
A	AT	AU95	Gerlostal Roller	47.19136	12.00737	25	2.297	0.584	25	0.823	
A	AT	AU96	Gesaeuse	47.56942	14.66103	25	2.177	0.549	25	0.887	2
A	AT	AU97	Gosau Seekaralm	47.54148	13.54166	15	2.232	0.540	15	0.907	1
A	AT	AU98	Patscherkofel	47.21301	11.46312	25	2.204	0.506	25	0.895	
A	AT	AU99	Kaunertal	46.92558	10.74445	25	2.117	0.520	25	0.933	
A	AT	AU100	Kuehtai	47.22077	11.03954	25	2.118	0.488	25	0.743	
A	AT	AU101	Madlriegel	47.32408	14.64619	25	2.062	0.571	25	0.827	
A	AT	AU102	Oberhauser Zirmwald	46.95050	12.21081	25	2.284	0.512	25	0.823	1
A	AT	AU103	Stadl Mur Paal	47.03722	14.03319	25	2.115	0.616	25	0.867	
A	AT	AU104	PetzenKrischa	46.51069	14.75872	25	2.258	0.534	25	0.880	
A	AT	AU105	Stoderzinken	47.45864	13.81461	25	2.038	0.515	25	0.827	1
A	AT	AU106	Stubachtal	47.15676	12.62333	25	2.149	0.599	25	0.833	1
A	AT	AU107	Sumperboden	47.60894	14.11114	25	2.215	0.581	25	0.860	1
A	AT	AU108	Wurzeralm	47.64769	14.25972	25	2.315	0.555	25	0.943	
A	AT	AU109	Schlegeissperre	47.03028	11.69523	25	2.231	0.518	25	0.883	
A	AT	AU110	Zirbitzkogel Sabathygebiet	47.07794	14.58302	25	2.155	0.544	25	0.867	
A	AT	AU111	Zirbitzkogel Rothaidenweg	47.07511	14.59516	23	2.187	0.570	23	0.903	
A	AT	AU112	Sturzelbach Rieder Höhe	46.75532	12.61145	25	2.265	0.579	25	0.901	
A	CH	CH113	Moosalp	46.25935	7.82682	24	2.189	0.536	24	0.877	
A	AT	AU114	Dachstein High	47.51667	13.86667	16	2.296	0.577	16	0.850	
A	AT	AU115	Dachstein Low	47.53056	13.91250	16	2.183	0.536	16	0.858	1
A	DE	DE116	Berchtesgaden	47.49278	12.94806	16	2.206	0.550	16	0.875	
A	AT	AU128	Neukirchen	47.29461	12.21026	23	2.310	0.571	24	0.768	2
A	FR	FR129	Chamrousse	45.12711	5.89405	20	2.239	0.587	20	0.732	
A	FR	FR130	Dormillouse	44.38961	6.39855	20	2.182	0.478	20	0.747	
A	IT	IT131	Pila	45.68638	7.33383	24	1.866	0.513	24	0.645	

A	CH	CH132	Grächen	46.19908	7.84875	12	2.325	0.509	12	0.455	
A	CH	CH133	Turtmann	46.21403	7.71451	12	2.091	0.555	12	0.318	
A	FR	FR135	Magland	45.99879	6.70615	24	2.025	0.549	24	0.732	
A	FR	FR136	La Clusaz	45.89458	6.46612	10	2.130	0.528	10	0.467	
A	FR	FR137	Les Allues	45.36318	6.58825	26	2.264	0.529	26	0.652	
A	FR	FR138	Allevard	45.38945	6.13959	24	2.107	0.447	24	0.779	
A	FR	FR139	Saint-Firmin	44.81694	6.03931	33	2.236	0.451	33	0.833	
A	FR	FR140	Bramans	45.18319	6.82863	24	2.155	0.549	24	0.794	
A	FR	FR141	Bourg St. Maurice	45.57434	6.83790	24	2.149	0.531	24	0.609	
A	IT	IT142	Mazzo di Valtellina	46.25251	10.30436	24	1.993	0.511	24	0.819	
A	IT	IT143	Laghi Gemelli	45.99655	9.80084	32	2.111	0.523	32	0.389	
A	IT	IT144	Lago Fregiabolgia	46.02344	9.85411	11	2.071	0.547	11	0.618	
A	IT	IT145	Valtournenche	45.81137	7.53695	17	2.172	0.543	17	0.228	
A	IT	IT146	Cogne	45.59781	7.36461	20	2.061	0.520	20	0.763	
A	*Total*					*2766*			*2767*		*21*
C	PL	PO117	Morskie Oko	49.20000	20.08000	11	1.969	0.604	10	0.844	
C	SK	SK118	Velka Studena Dolina	49.17000	20.20000	17	2.010	0.625	17	0.949	1
C	UK	UK119	Kedryn Forest Reserve	48.42000	24.00000	17	1.828	0.555	16	0.783	
C	RO	RO120A	Borsa (autochthonous)[4]	47.58000	24.63000	5	1.947	0.541	5	0.600	
C	RO	RO121	Neagra Sarului	47.17000	25.28000	19	2.066	0.648	19	0.883	2
C	RO	RO122	Negoiu	47.10000	25.20000	17	2.154	0.562	17	0.816	
C	RO	RO123	Cindrel	45.58000	23.80000	7	2.121	0.613	7	0.810	
C	RO	RO124	Gentiana	45.38000	22.87000	7	2.131	0.603	7	0.810	
C	RO	RO125	Gemenele	45.37000	22.83000	16	2.129	0.595	16	0.917	2
C	RO	RO126	Muntinul Mare	45.36217	23.67667	25	2.152	0.518	25	0.727	1
C	RO	RO127A	Valea Lala (autochthonous)[4]	47.53806	24.69722	19	2.133	0.616	19	0.854	
C	RO	RO147	Urdele	45.35000	23.67837	24	2.119	0.536	24	0.750	
C	RO	RO148	Piciorul Plescutei	47.55295	24.92163	6	2.068	0.564	6	0.867	
C	SK	SK149	Srbské Pleso	49.13961	20.07193	33	2.405	0.620	33	0.869	2
C	*Total*					*223*			*221*		*8*
Total						**2989**			**2988**		

n = sample size; A_R = allelic richness, H_E = expected heterozygosity, H = haplotypic diversity, A_p = number of population-specific haplotypes

[1] A = European Alps, C = Carpathians

[2] AT = Austria, CH = Switzerland, FR = France, DE = Germany, IT = Italy, PL = Poland, RO = Romania, SK = Slovakia, UK = Ukraine

[3] 2 individuals, identified as putative *Pinus peuce,* were excluded in DE80 (unpubl. data)

[4] several individuals identified as putative *Pinus sibirica* were excluded in RO120 and RO127 (Lendvay et al., 2014)

Lab procedures

Sampled needles were kept fresh, frozen, lyophilised, or in silica gel before disruption in 2-mL tubes or 96-well plates using a Mixer Mill MM300 (Retsch, Haan, Germany). Optimally, fresh needles were cut into pieces and lyophilised shortly after sampling in the field, while drying needles on silica-gel gave low DNA yield.

The 11 nSSRs and 4 cpSSRs were genotyped in three multiplex PCRs, following the methods described in Lendvay et al. (2014). All pertinent information on primers can be found in Table S1.2.

Few individuals were subsequently removed from the total sample on the basis of their genotypes, as they were identified as putatively *Pinus sibirica* (n=15; Lendvay et al., 2014), and possibly planted *Pinus peuce* (n=2; unpubl. data). Further samples were excluded because of genotyping failure,

Table S1.2 Technical information on the nuclear and chloroplast microsatellite markers (simple-sequence repeats, SSRs).

				Primer information					
Genome	Original reference	Locus	MP[1]	Forward (5'→3')	Conc. [µM]	Dye	Reverse (5'→3')	Conc. [µM]	Sizes [bp]
Nuclear	Salzer et al. (2009)	Pc7	1	TGGTCATGTTTCCTTATCAATTC	0.25	FAM	TCGCAAACCATCTATTGACC	0.25	342-402
		Pc1b	1	CCACCATCTTGTTTTTGTGTTC	0.2	FAM	TTCTCTCCACCCAGCCTAAA	0.2	164-222
		Pc23	1	GGGCATCATTATTTTCTTACAA	0.2	VIC	CTTGATATACCATGCCACAACC	0.2	195-285
		Pc18	1	TTCCCAAAGACCATAGAACCA	0.2	NED	TCATGAAATATTACGTCCCTTATCC	0.2	144-162
		Pc22	1	TGTCCCCAGATGTAGTATAATCAA	0.4	PET	GGTTCAACCCACCCATTCT	0.2	325-384
		Pc35	1	CCCCTCGATTCGAAAATGAT	0.2	PET	TTGGAATGTTGCAGTCCTGA	0.2	162-165
	Lendvay et al. (2014)	28Z	2	AGTTGACTGTGCCGTCATATTG	0.08	FAM	CGCATTCCCTAATGCCAAGC	0.08	288-324
		BUG	2	CTTCAATGCGGCTTCAGAAT	0.1	FAM	GAGTAGAAGAACAAGTTCTAAGTTTGG	0.1	101-133
		HJM	2	GAAAGGTCACATGTTGCACG	0.03	FAM	CACATTCTCCAGAGCACTCC	0.03	168-199
		YAU	2	TCCTTGCCTCATTTTCATCG	0.1	ATTO550	AGCACAGTGAAGGTCACAGC	0.1	144-165
		CQG	2	TGTCATGAAGAAATAACCAGGAGA	0.1	Yakima Yellow	TTCCTAGTTTGGTGTGTGGTTG	0.1	169-179
Chloroplast	Vendramin et al. (1996)	Pt15169	3	CTTGGATGGAATAGCAGCC	0.127	FAM	GGAAGGGCATTAAGGTCATTA	0.127	131-141
		Pt26081	3	CCCGTATCCAGATATACTTCCA	0.169	HEX	TGGTTTGATTCATTCGTTCAT	0.169	105-109
		Pt36480	3	TTTTGGCTTACAAAATAAAAGAGG	0.212	HEX	AAATTCCTAAAGAAGGAAGAGCA	0.212	147-151
		Pt63718	3	CACAAAAGGATTTTTTTTCAGTG	0.064	FAM	CGACGTGAGTAAGAATGGTTG	0.064	91-98

[1] MP = Multiplex PCR mix

Annealing Temperatures and commercial PCR mixes used:
Multiplex 1: 54˚C, Multiplex PCR Kit (QIAGEN, No. 206145)
Multiplex 2: 58˚C, Type-it Microsatellite PCR Kit (QIAGEN, No.206243)
Multiplex 3: 55˚C, Multiplex PCR Kit (QIAGEN, No. 206145)

PCR fragments were electrophoretically separated on an automated capillary sequencer (ABI 3100 and 3130; Applied Biosystems, Foster City), and using GeneMapper 3.7 and 5.0 (Applied Biosystems) for visual allele calling.

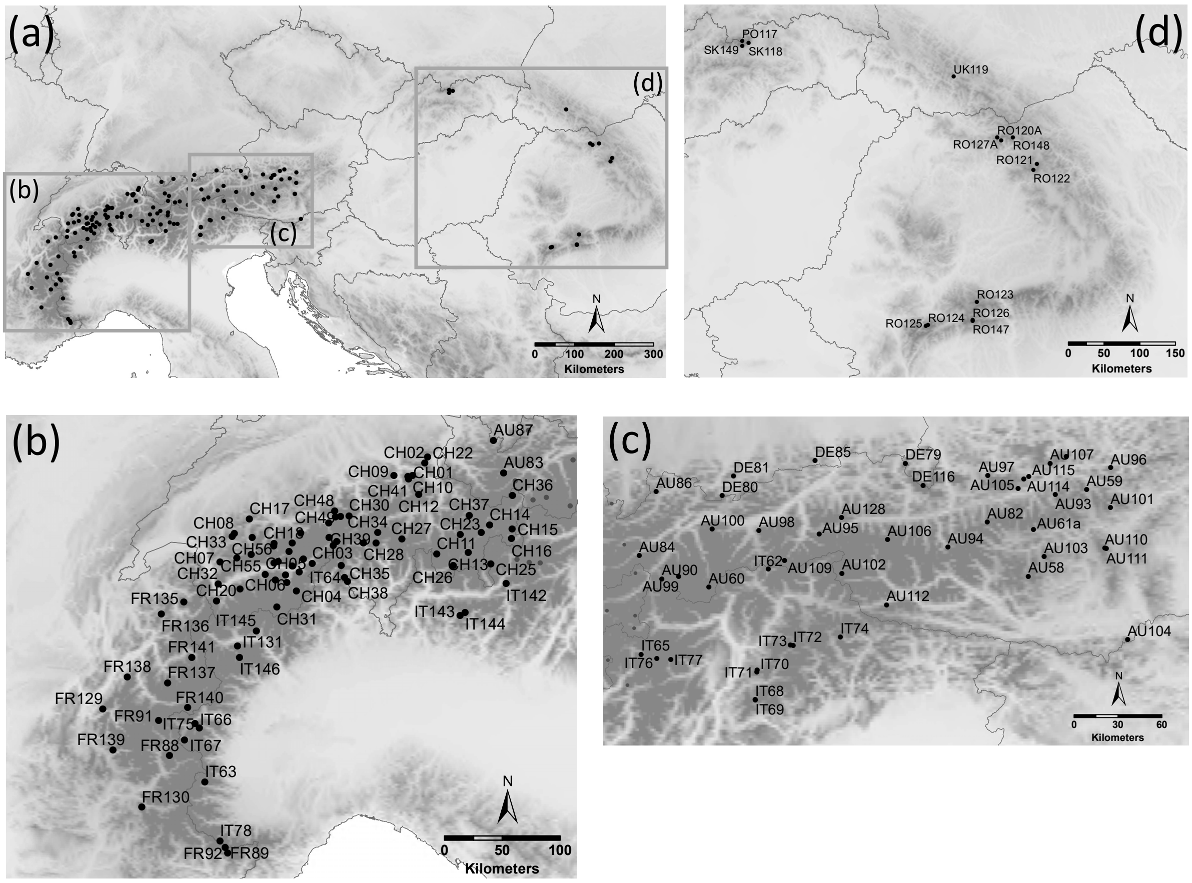

FIGURE S1.1 Locations of the 147 *Pinus cembra* stands sampled across the species' range. (a) Full natural range and sampled locations (black dots); populations labelled for (b) western Alpine, (c) eastern Alpine, and (d) Carpathian ranges; codes are detailed in Table S1.1, grey dots in (b) and (c) mark unlabelled populations.

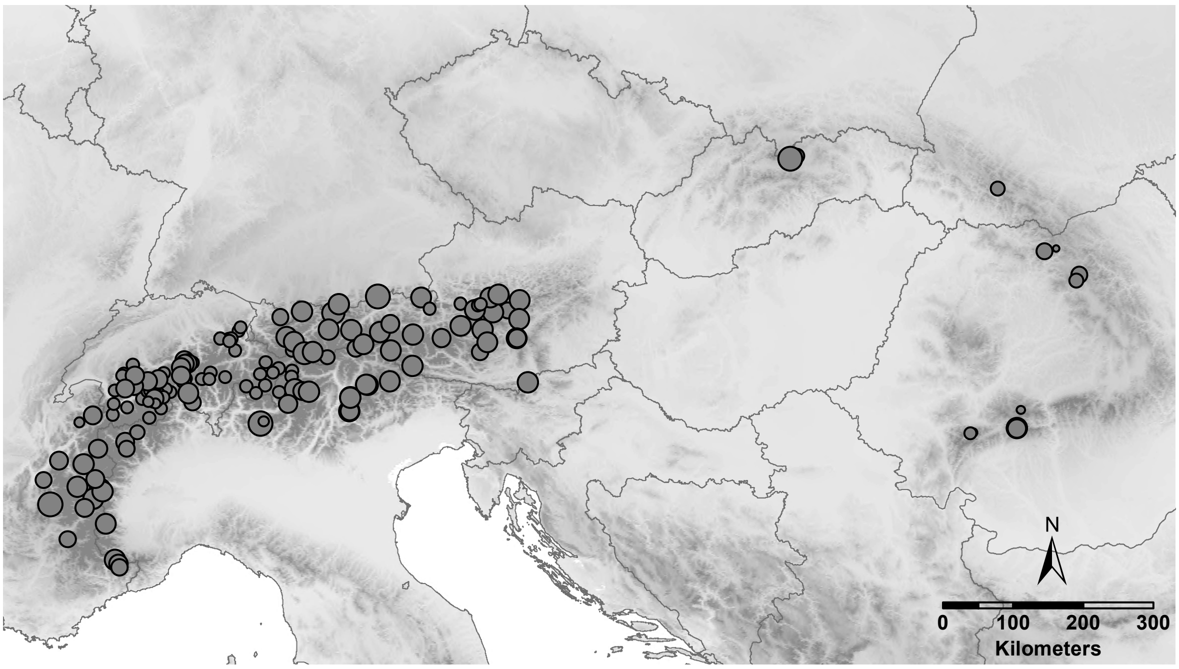

FIGURE S1.2 Sample sizes, indicated by circle sizes, of the 147 *Pinus cembra* stands sampled across the species' range; precise numbers are given in Table S1.1.

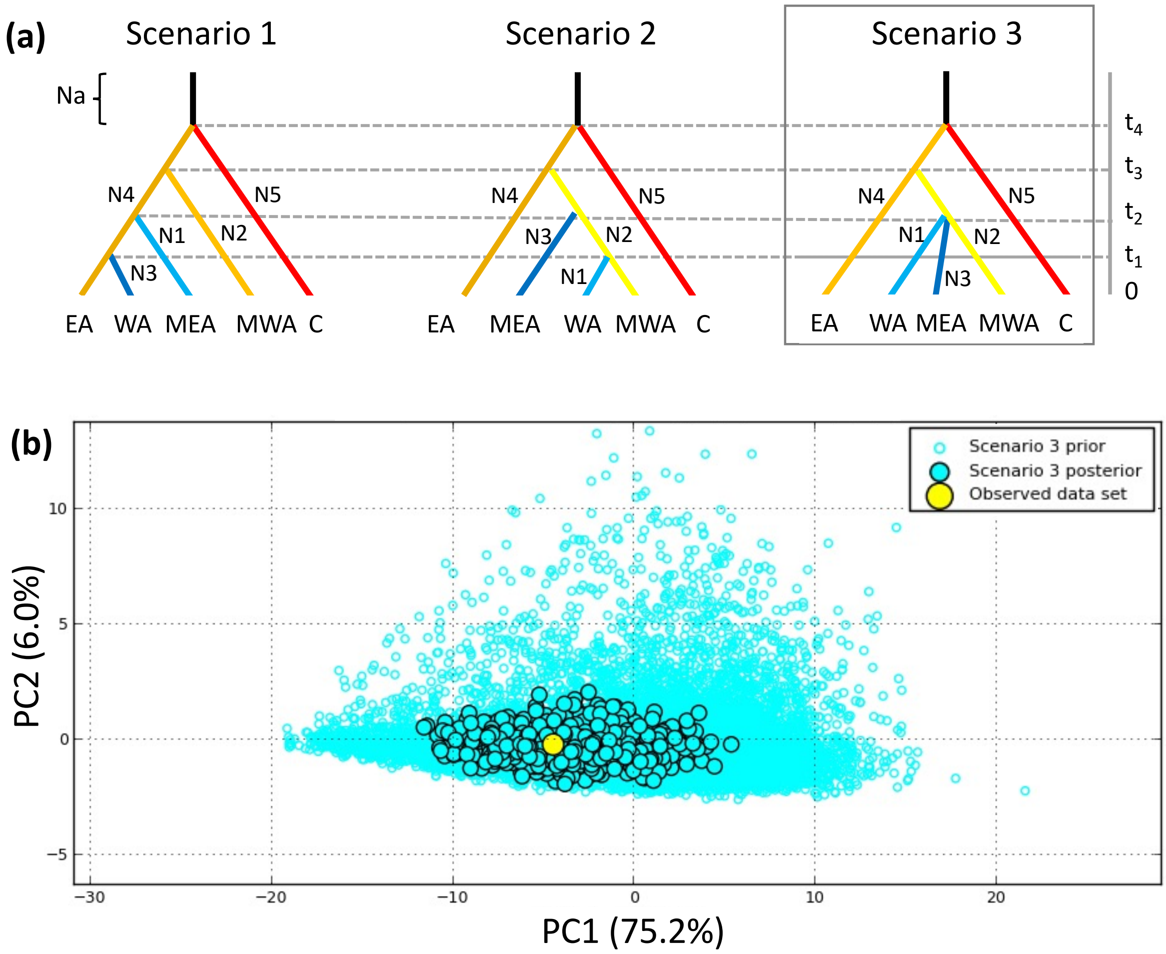

FIGURE S1.3 (a) Alternative demographic scenarios S1-S3 tested in the Approximate Bayesian Computation analyses (Cornuet et al., 2014). Nx refers to respective population sizes, with Na being the ancestral population size; t_1-t_4 mark time points of the separation of genetic clusters; regional genetic clusters refer to Carpathians (C), Eastern Alps (EA), Mid-Eastern Alps (MEA), Mid-Western Alps (MWA) and Western Alps (WA), following the population assignment by STRUCTURE at $K = 5$ (Fig. S2.4d). (b) Principal component analysis (PCA) of summary statistics based on 10,000 simulated datasets in DIYABC (scenario 3), with first two principal components (PCs) displayed

Appendix 2 Genetic structure in *Pinus cembra* from the European Alps and the Carpathians, based on nuclear and chloroplast microsatellite markers (simple-sequence repeats, n/cpSSRs), and demographic analyses using nSSRs.

Assessment of spatial genetic structure

In STRUCTURE v. 2.3.4 (Pritchard et al., 2000), we chose the LOCPRIOR model (Hubisz et al., 2009) together with the admixture and correlated allele frequencies options, given the low level of genetic differentiation and preliminary trials. We ran 1,000,000 Markov Chain Monte Carlo repetitions discarding 100,000 burn-in repetitions, with all other parameters set to default values. For *K* = 1-10, we performed 10 iterations at each value of *K* and the results were summarised using STRUCTURE HARVESTER v. 0.6.94 (Earl & vonHoldt, 2012). For subsequent grouping of populations (e.g. demographic analysis), we used the plot of LnP(*D*) as a function of *K* values to find the number of genetic clusters that best explains our data, as described in the STRUCTURE documentation, accounting for the increasing sub-structuring with increasing *K* (Janes et al., 2017). For visualisation, we subjected the STRUCTURE output files to the *greedy* algorithm in CLUMPP (Jakobsson & Rosenberg, 2007), as implemented in CLUMPAK (Kopelman et al., 2015), and used this output for generating GIS-based maps in ArcMap v. 10.8.1.14362 (ESRI Inc.).

For the analysis of cpSSR haplotypes, we used BAPS v. 6.0 (Corander et al., 2003) with individuals also grouped according to their populations. We applied admixture analysis with linked loci and repeated the analysis 10 times for each *K* = 2-10. The most probable number of *K* was chosen based on the highest value of log(marginal likelihood). To assign each population to the genetic clusters, we repeated the analysis 100 times at the most probable *K* value. We then visualised the spatial distribution of cpSSR-based genetic clusters across the species' range using ArcMap (ESRI Inc.).

To explore genotypic variation across all individuals, and given the low population differentiation, we carried out a discriminant analysis of principal components (DAPC) using the *dapc* function of the ADEGENET R package v. 2.1.5 (Jombart, 2008), which transforms the uncorrelated principal components and generates synthetic discriminant axes that maximise between-population variation while minimising within-population variation (Jombart et al., 2010). We conducted the DAPC with the population of each individual as prior information and used the *optim.a.score* function to define the optimal number of principal components (PCs) to retain based on the α-score statistics to avoid over-fitting problems.

To test for isolation by distance, using geographic and linearised genetic distances F_{ST} / (1 - F_{ST}) (Rousset, 2000), we ran 999 permutations in a Mantel test with the VEGAN R package v. 2.5-7 (Oksanen et al., 2020). Geographic distances were calculated from latitude and longitude data of centroid populations with the *distm* function of the GEOSPHERE R package v. 1.5.14 (Hijmans et al., 2021), and genetic distances were calculated based on pairwise F_{ST} values (Weir & Cockerham, 1984) as implemented with the *genet.dist* function of the HIERFSTAT R package v. 0.5-10 (Goudet, 2005).

Demographic analysis

We inferred the demographic history of Swiss stone pine using Approximate Bayesian Computation (ABC; Beaumont et al., 2002) implemented in DIYABC 2.0 (Cornuet et al., 2014), relying on the K = 5 genetic clusters identified in the STRUCTURE analysis (see above): Carpathians (C), Eastern Alps (EA), mid-Eastern Alps (MEA), mid-Western Alps (MWA) and Western Alps (WA). Given the high level of genetic admixture within each cluster, the DIYABC analysis only considered individuals with assignment probabilities of q ≥ 0.6 (n = 1876), among which we randomly selected 50 individuals for demographic inference. We consider this data restriction as a measure to limit the violation of model assumption (no gene flow), at the cost of simplification. The genetic diversity parameters of the five genetic clusters indicated a westward cline of decreasing diversity, which might be indicative of a colonisation pattern; therefore, we took this into account when designing the demographic scenarios.

A set of pilot simulations, performed to select the three final competing scenarios, highlighted a good support for an ancient divergence of clusters C and EA from a common ancestor at time t_4, and a subsequent divergence of MWA from EA at time t_3. The three final scenarios tested thus differed only in the splitting times of WA and MEA from MWA as follows (Fig. S1.3a): S1) WA and MEA split from MWA at time t_2 and t_1 respectively; S2) MEA and WA split from MWA at time t_2 and t_1 respectively; S3) MEA and WA split from MWA at time t_2. In all scenarios, t# refers to time scale (scaled by generation time) and N# refers to effective population size of the corresponding populations (i.e., C, EA, MEA, MWA, WA and ancestral population “a”) during each time period.

For all simulations, the Generalised Stepwise Mutation model (GSM; Estoup et al., 2002) with Single Nucleotide Indels (SNI) was used. Default priors were changed to obtain better posterior distributions based on the results from the pilot runs (Table S2.1). The minimum and maximum priors for SSR mutation rate were set to $1×10^{-5}$–$7×10^{-4}$, respectively. The mean number of alleles (*A*) and mean expected heterozygosity (H_E) were used as summary statistics for single populations, and H_E, *A*, and the classification index for population pairs. For each scenario, a million simulations were performed, after which the most likely scenario was evaluated by comparing posterior probabilities, using logistic regression. Goodness-of-fit was assessed for each scenario by model checking using the principal component analysis (PCA) approach implemented in DIYABC, which measures the discrepancy between simulated and empirical data. To date the demographic history, we assumed a generation time of 40 years (Ulber et al., 2004).

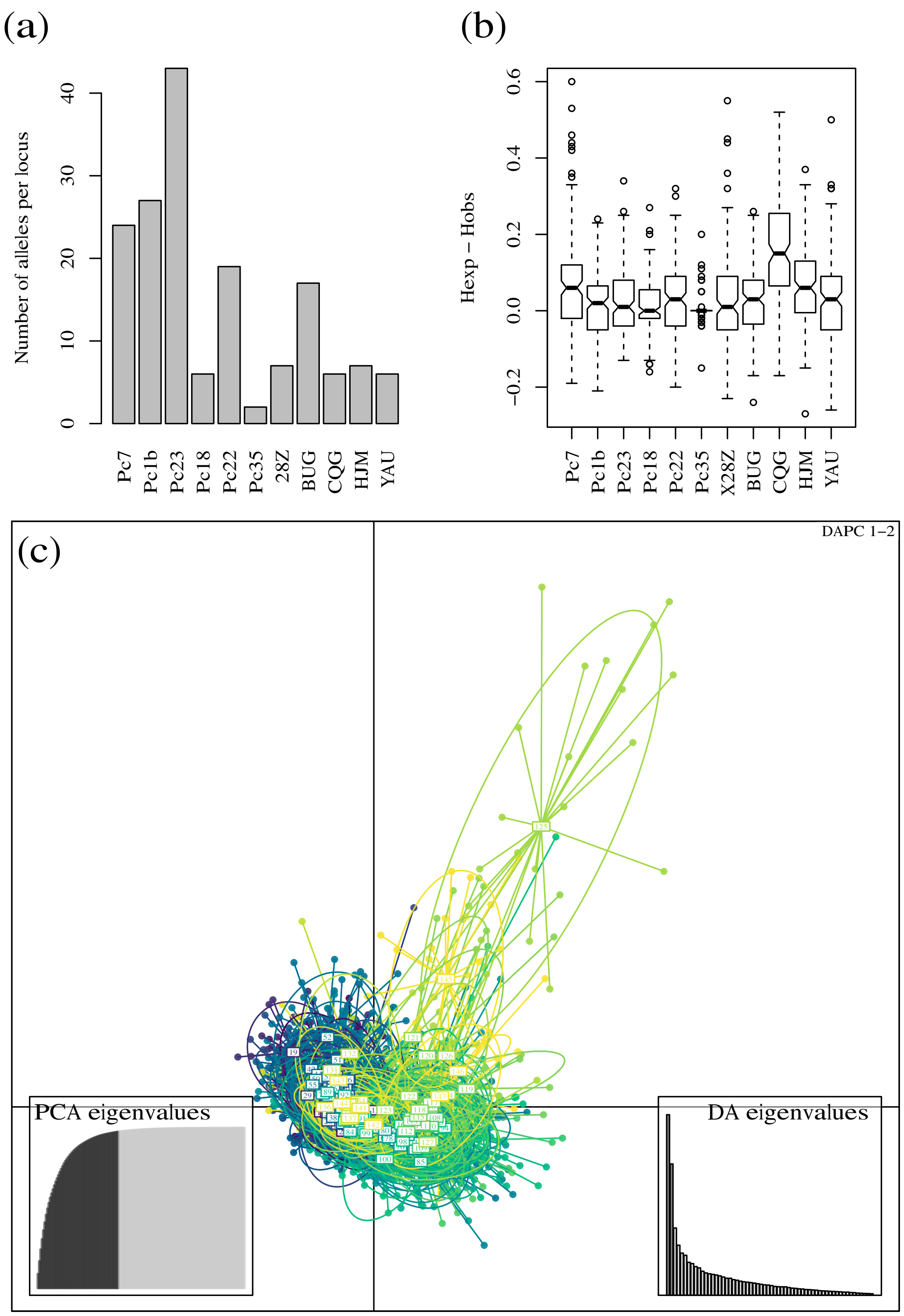

Figure S2.1 (a) Number of alleles and (b) difference between expected (H_E) and observed heterozygosity (H_O) per nuclear microsatellite (simple-sequence repeat, nSSR) locus, calculated across all samples. (c) Genotypic variation of individuals based on their nSSRs, using a discriminant analysis of principal components (DAPC). The first two discriminant functions displayed summarise 16.4% and 11.9% of the total variance, respectively. The outlier population at the top right (labelled 125) refers to Muntinul Mare (RO126; see Table S1.1).

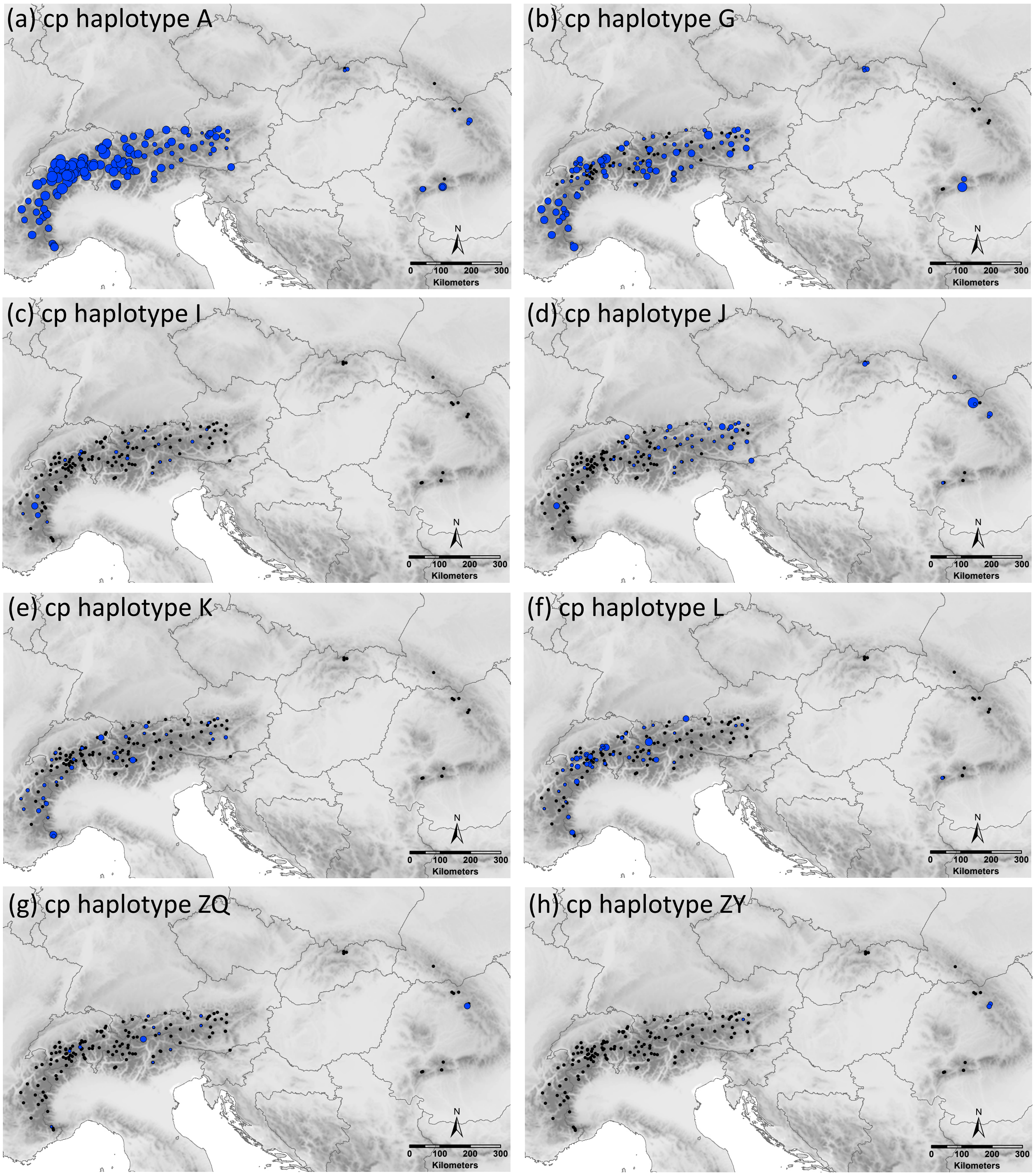

FIGURE S2.2 (a-h) Exemplary chloroplast haplotype distributions of *Pinus cembra* from the European Alps and the Carpathians. Coloured circles symbolise haplotype frequencies normalised for sample size per population, black dots indicate stands without respective haplotype occurrence.

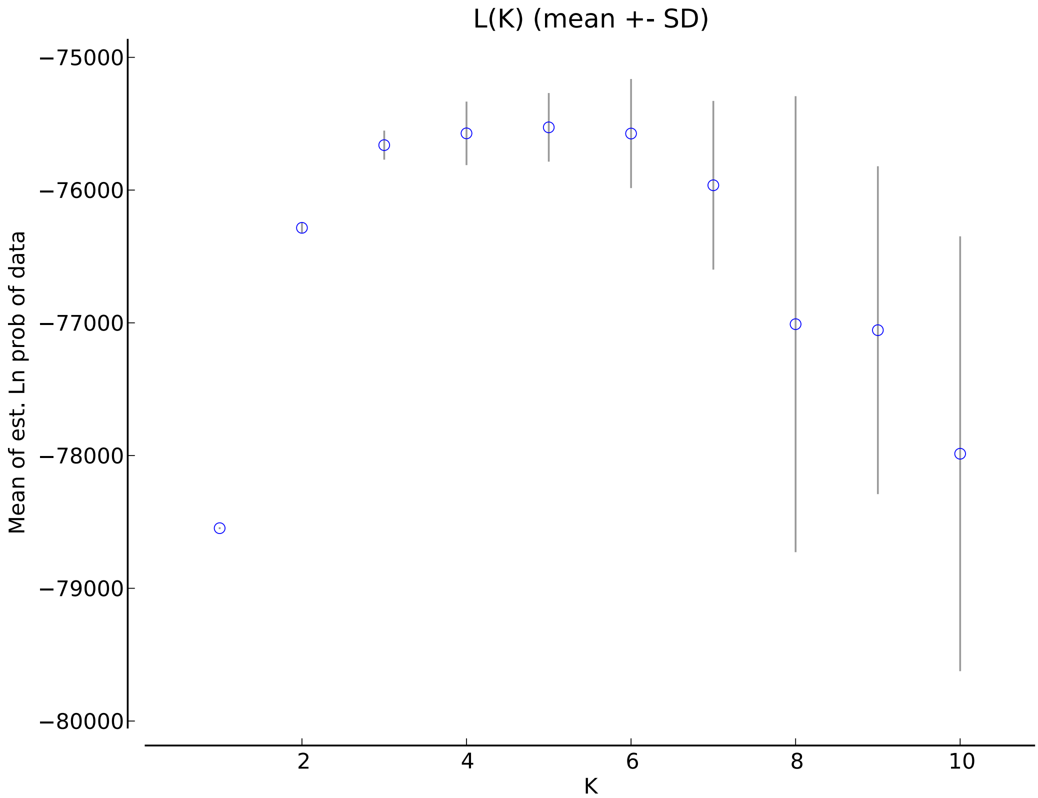

FIGURE S2.3 Likelihood LnP(D), giving the mean and the variance over 10 iterations, as a function of the increasing number of genetic clusters *K* = 1-10 in the Bayesian analysis using STRUCTURE (Hubisz et al., 2009; Pritchard et al., 2000), as determined by STRUCTURE HARVESTER (Earl & vonHoldt, 2012), for nuclear microsatellite (simple-sequence repeat, SSR) data of *Pinus cembra* from the European Alps and the Carpathians.

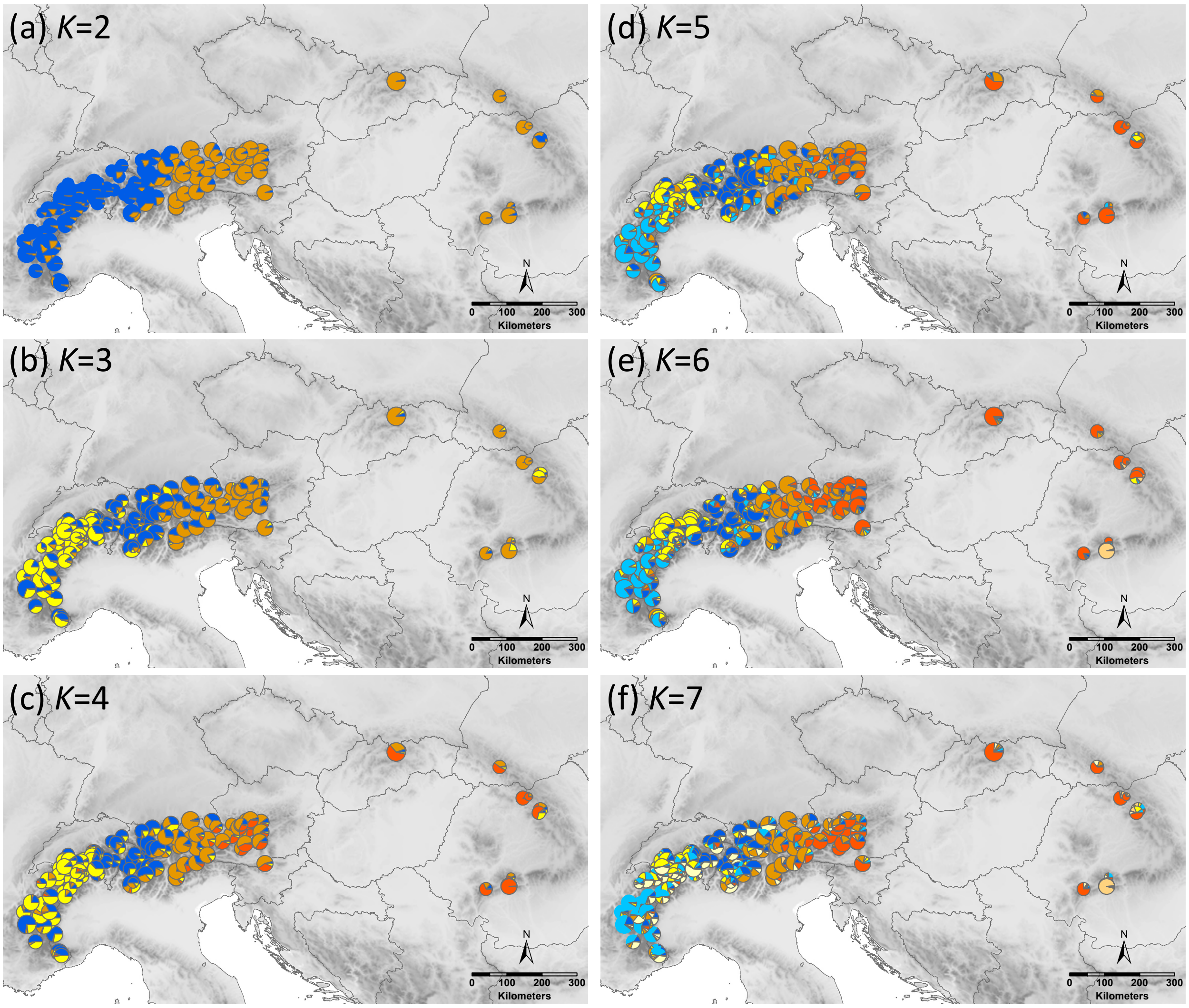

FIGURE S2.4 Population-wise assignment probabilities for *K* = 2–7 inferred by the Bayesian analysis of cluster assignment using STRUCTURE (Hubisz et al., 2009; Pritchard et al., 2000), as determined by STRUCTURE HARVESTER (Earl & vonHoldt, 2012), for nuclear microsatellite (simple-sequence repeat, nSSR) data of *Pinus cembra* stands from the European Alps and the Carpathians. Probabilities are means over 10 iterations, as determined in CLUMPP (Jakobsson & Rosenberg, 2007). Circle sizes indicate sample numbers.

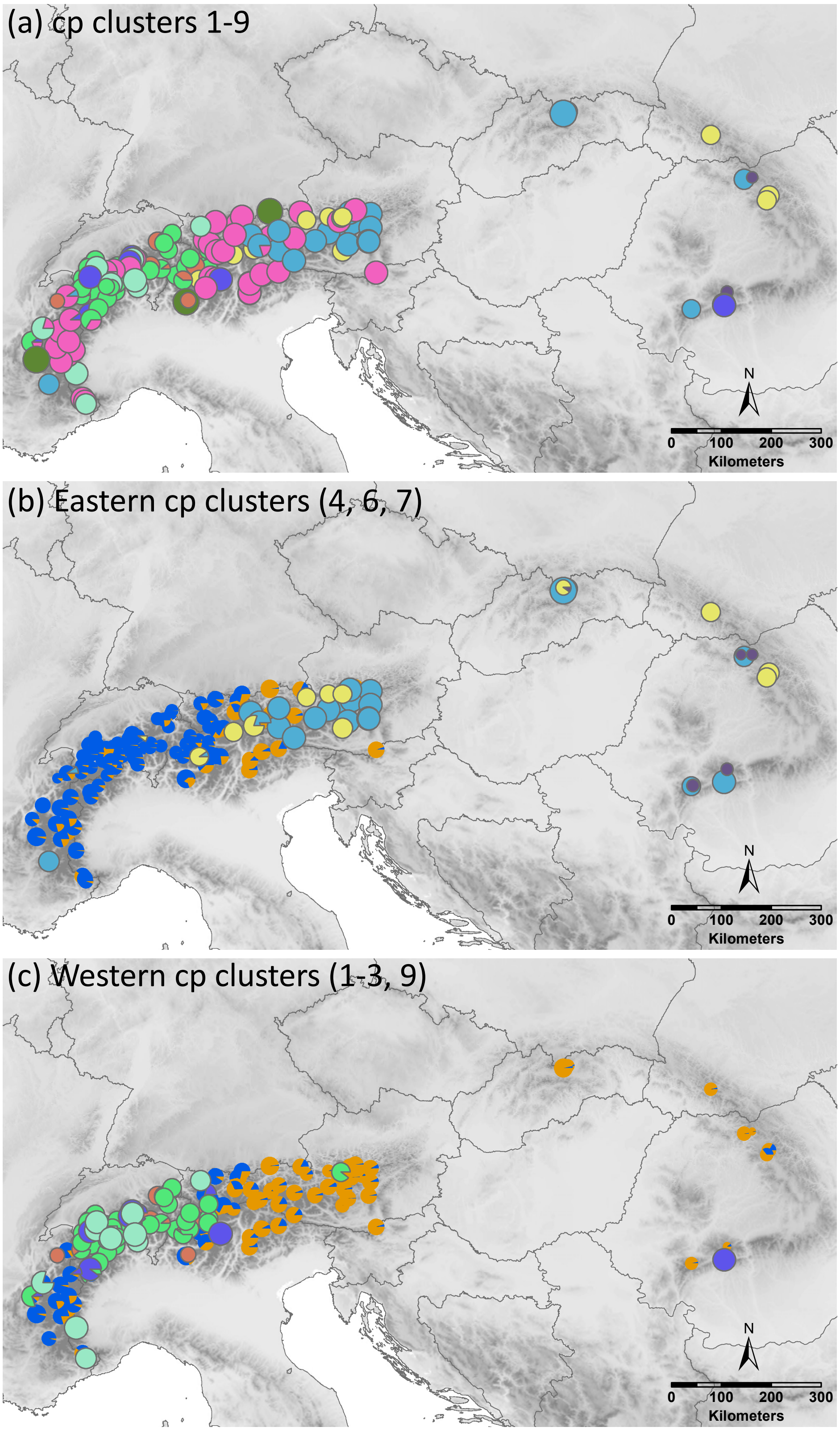

FIGURE S2.5 Population-wise assignment probabilities for *K* = 9 inferred by the Bayesian analysis of clustering using BAPS (Corander et al., 2003) for chloroplast microsatellite (simple-sequence repeat, cpSSR) data of *Pinus cembra* stands from the European Alps and the Carpathians. (a) All populations (cf. Fig. 2b in main text), (b) clusters 4, 6 and 7 predominantly occurring in the eastern part of the range, (c) clusters 1-3 and 9, largely restricted to the western part of the range. STRUCTURE results for *K* = 2 based on nuclear microsatellite (nSSR) data are given as small pie charts in the background in (b) and (c) to relate cpSSR haplotype distribution to that of the two main nSSR clusters (Fig. S2.4a). Circle sizes indicate sample numbers.

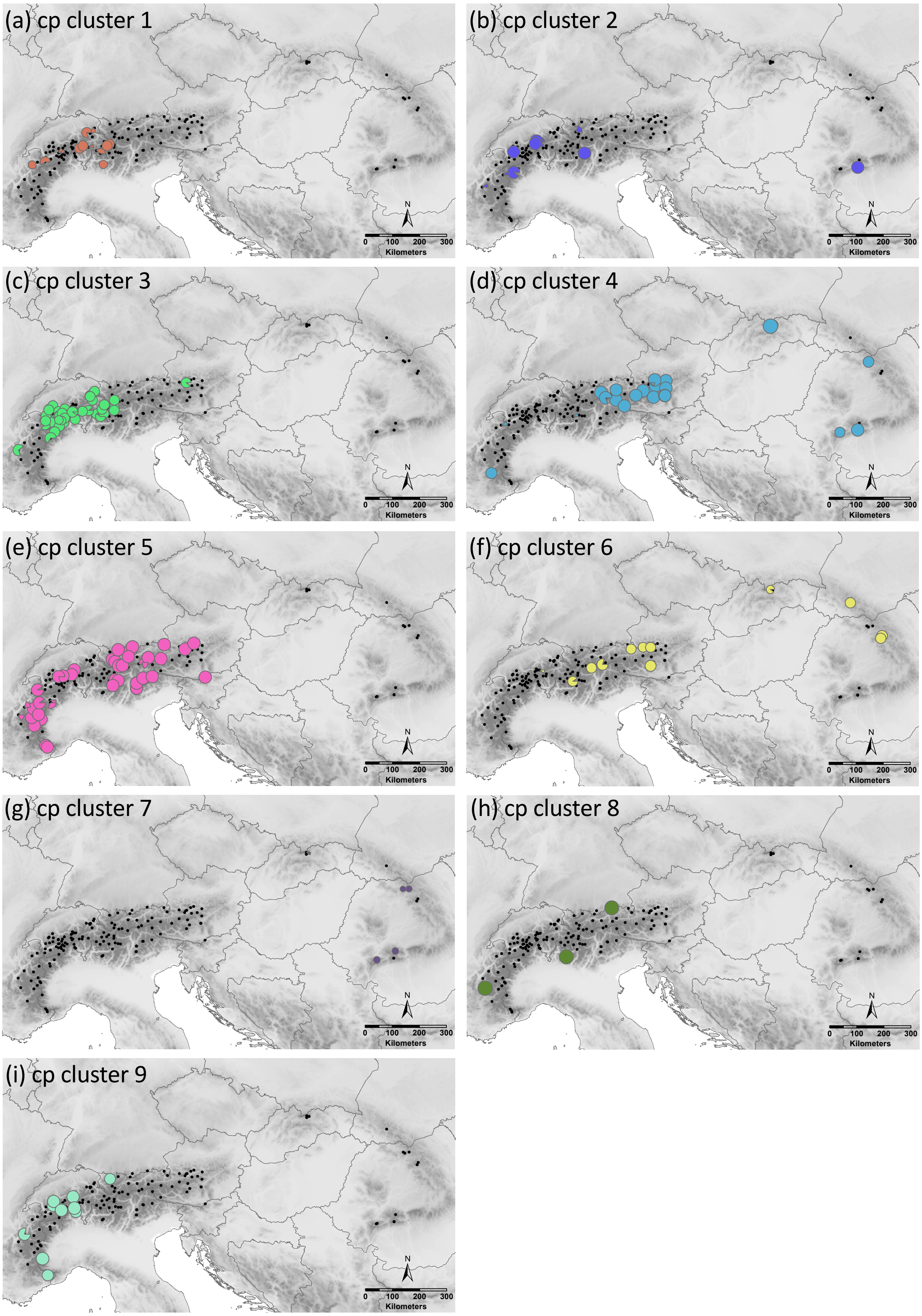

FIGURE S2.6 (a-i) Population-wise assignment probabilities for individual genetic clusters at *K* = 9 inferred by the Bayesian analysis of cluster assignment using BAPS (Corander et al., 2003) for chloroplast microsatellite (simple-sequence repeat, cpSSR) data of *Pinus cembra* stands from the European Alps and the Carpathians. Circle sizes indicate sample numbers. Coloured circles or fractions refer to respective genetic cluster, black circles indicate remaining sampled populations.

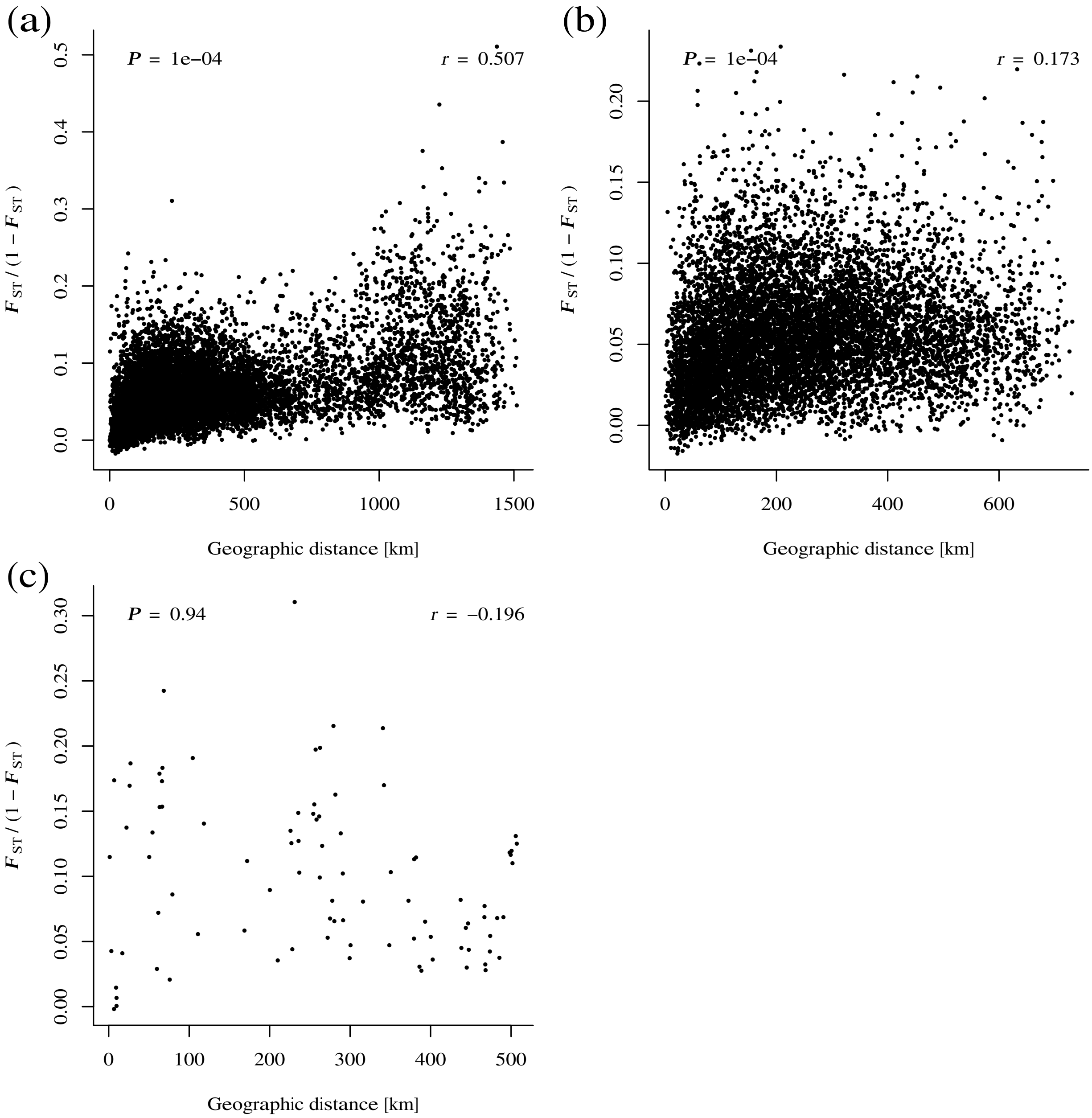

Figure S2.7 Patterns of isolation by distance using linearized pairwise genetic (F_{ST}) and geographic distances (km) between *Pinus cembra* stands from (a) both the European Alps and the Carpathians, (b) the European Alps only, and (c) the Carpathians only. The Mantel correlations are highly significant for (a) and (b) (range-wide: $p < 0.001$, $r = 0.507$; Alps: $p < 0.001$, $r = 0.173$), but not for (c) (Carpathians: $p = 0.94$, $r = -0.196$).

Table S2.1 Analysis of molecular variance (AMOVA) for partitioning total genetic variation among regions (Alps *vs.* Carpathians, East vs. West according to STRUCTURE clustering at $K = 2$), among populations within regions, and within populations

			Alps vs. Carpathians		East vs. West	
Markers	**Source of variation**	**df**	**% variation**		**% variation**	
nSSRs	Among regions (F_{CT})	1	2.87***		2.23***	
	Among populations (F_{SC})	145	5.37***		4.79***	
	Within populations	5831	91.75***		92.98***	
	Overall F_{ST}			0.082***		0.070***
cpSSRs	Among regions (F_{CT})	1	6.15***		4.66***	
	Among populations (F_{SC})	145	5.87***		4.71***	
	Within populations	2841	87.98***		90.63***	
	Overall F_{ST}			0.120***		0.094***

*** = $p < 0.001$; nuclear and chloroplast microsatellites (simple-sequence repeats; nSSRs and cpSSRs), respectively; degrees of freedom (df)

Table S2.2 Posterior probability of each of the three tested scenarios and their 95% confidence intervals (CI) based on the logistic estimate according to DIYABC (Cornuet et al., 2014).

Scenario	Posterior probability	95% CI (lower-upper)
1	0.2102	0.1511-0.2693
2	0.0994	0.0672-0.1317
3	0.6903	0.6274-0.7532

Table S2.3 Estimation of parameters of the best scenario based on local linear regression using DIYABC (Cornuet et al., 2014).

Parameter	Mean	Median	Mode	Quantile			
				2.50%	5%	95%	97.50%
N1	1.64E+04	1.45E+04	8.86E+03	3.23E+03	4.14E+03	3.48E+04	3.73E+04
N2	7.42E+03	6.66E+03	4.77E+03	1.89E+03	2.42E+03	1.54E+04	1.72E+04
N3	9.02E+03	8.37E+03	6.47E+03	2.16E+03	2.81E+03	1.74E+04	1.86E+04
N4	2.95E+04	2.94E+04	3.04E+04	1.15E+04	1.39E+04	4.59E+04	4.79E+04
N5	4.95E+04	4.98E+04	5.11E+04	1.88E+04	2.27E+04	7.55E+04	7.77E+04
t_1	6.60E+02	6.31E+02	6.29E+02	1.33E+02	1.94E+02	1.21E+03	1.36E+03
t_2	1.65E+03	1.63E+03	1.58E+03	5.06E+02	6.33E+02	2.74E+03	2.86E+03
t_3	5.25E+03	5.31E+03	5.27E+03	2.23E+03	2.76E+03	7.50E+03	7.74E+03
Na	4.82E+02	4.72E+02	1.99E+02	3.31E+01	5.66E+01	9.44E+02	9.72E+02
µmic_1	1.42E-04	1.24E-04	1.08E-04	5.69E-05	6.43E-05	2.87E-04	3.45E-04
pmic_1	2.40E-01	2.49E-01	3.00E-01	1.30E-01	1.45E-01	3.00E-01	3.00E-01
snimic_1	2.13E-06	1.15E-06	1.40E-08	1.73E-08	2.71E-08	7.38E-06	8.46E-06

Table S2.4 Model checking for the best scenario (S3; see Fig. 2d in main text) of DIYABC analysis (Cornuet et al., 2014).

Summary statistics	Observed value	Proportion (simulated<observed)
Mean number of alleles in WA	5.6364	0.426
Mean number of alleles in MWA	5.4545	0.526
Mean number of alleles in MEA	5.3636	0.439
Mean number of alleles in EA	6.6364	0.4365
Mean number of alleles in C	7.6364	0.6155
Mean expected heterozygosity in WA	0.4942	0.2355
Mean expected heterozygosity in MWA	0.5378	0.4405
Mean expected heterozygosity in MEA	0.5055	0.2985
Mean expected heterozygosity in EA	0.5412	0.2965
Mean expected heterozygosity in EA	0.6102	0.559
Mean number of alleles (WA&MWA)	6.5455	0.456
Mean number of alleles (WA&MEA)	6.5455	0.436
Mean number of alleles (WA&EA)	7.9091	0.5315
Mean number of alleles (WA&C)	8.6364	0.5955
Mean number of alleles (MWA&MEA)	6.2727	0.4175
Mean number of alleles (MWA&EA)	7.5455	0.4735
Mean number of alleles (MWA&C)	8.3636	0.57
Mean number of alleles (MEA&EA)	7.5455	0.453
Mean number of alleles (MEA&C)	8.3636	0.556
Mean number of alleles (EA&C)	8.7273	0.511
Mean expected heterozygosity (WA&MWA)	0.532	0.3665
Mean expected heterozygosity (WA&MEA)	0.5125	0.2805
Mean expected heterozygosity (WA&EA)	0.5297	0.2645
Mean expected heterozygosity (WA&C)	0.5766	0.4205
Mean expected heterozygosity (MWA&MEA)	0.5418	0.402
Mean expected heterozygosity (MWA&EA)	0.5563	0.3765
Mean expected heterozygosity (MWA&C)	0.5884	0.474
Mean expected heterozygosity (MEA&EA)	0.5359	0.291
Mean expected heterozygosity (MEA&C)	0.5865	0.4585
Mean expected heterozygosity (EA&C)	0.5919	0.442
Classification index (WA&MWA)	0.9284	0.2935
Classification index (WA&MEA)	0.8932	0.2525
Classification index (WA&EA)	0.9513	0.2075
Classification index (WA&C)	1.0926	0.358
Classification index (MWA&WA)	0.9808	0.475
Classification index (MWA&MEA)	1.0016	0.4475
Classification index (MWA&EA)	1.1201	0.5005
Classification index (MWA&C)	1.2296	0.5775
Classification index (MEA&WA)	0.9375	0.397
Classification index (MEA&MWA)	0.9493	0.3345
Classification index (MEA&EA)	0.9422	0.2005
Classification index (MEA&C)	1.1802	0.515
Classification index (EA&WA)	1.0733	0.2915
Classification index (EA&MWA)	1.1419	0.3475
Classification index (EA&MEA)	1.0847	0.2695
Classification index (EA&C)	1.0656	0.3465
Classification index (C&WA)	1.424	0.6775
Classification index (C&MWA)	1.3965	0.548
Classification index (C&MEA)	1.4947	0.7335
Classification index (C&EA)	1.2663	0.6445

References

Corander, J., Waldmann, P., & Sillanpää, M. J. (2003). Bayesian analysis of genetic differentiation between populations. *Genetics, 163*, 367–374.

Cornuet, J.-M., Pudlo, P., Veyssier, J., Dehne-Garcia, A., Gautier, M., Leblois, R., … Estoup, A. (2014). DIYABC v2.0: a software to make approximate Bayesian computation inferences about population history using single nucleotide polymorphism, DNA sequence and microsatellite data *Bioinformatics, 30*, 1187–1189. doi:10.1093/bioinformatics/btt763

Earl, D. A., & vonHoldt, B. M. (2012). STRUCTURE HARVESTER: a website and program for visualizing STRUCTURE output and implementing the Evanno method. *Conservation Genetics Resources, 4*, 359–361. doi:10.1007/s12686-011-9548-7

Hubisz, M. J., Falush, D., Stephens, M., & Pritchard, J. K. (2009). Inferring weak population structure with the assistance of sample group information. *Molecular Ecology Resources, 9*, 1322–1332. doi:10.1111/j.1755-0998.2009.02591.x

Jakobsson, M., & Rosenberg, N. A. (2007). CLUMPP: a cluster matching and permutation program for dealing with label switching and multimodality in analysis of population structure. *Bioinformatics, 23*, 1801–1806. doi:10.1093/bioinformatics/btm233

Lendvay, B., Höhn, M., Brodbeck, S., Mindrescu, M., & Gugerli, F. (2014). Genetic structure in *Pinus cembra* from the Carpathian Mountains inferred from nuclear and chloroplast microsatellites confirms postglacial range contraction and identifies introduced individuals. *Tree Genetics & Genomes, 10*, 1419–1433. doi:10.1007/s11295-014-0770-9

Pritchard, J. K., Stephens, M., & Donnelly, P. (2000). Inference of population structure using multilocus genotype data. *Genetics, 155*, 945–959.

Salzer, K., Sebastiani, F., Gugerli, F., Buonamici, A., & Vendramin, G. G. (2009). Isolation and characterization of eight polymorphic nuclear microsatellite loci in *Pinus cembra* L. *Molecular Ecology Resources, 9*, 858–861. doi:10.1111/j.1755-0998.2008.02396.x

Vendramin, G. G., Lelli, L., Rossi, P., & Morgante, M. (1996). A set of primers for the amplification of 20 chloroplast microsatellites in Pinaceae. *Molecular Ecology, 5*, 595–598.

Appendix 3 Pollen and macrofossil records with respective geographic and temporal information, and list of references used to compile palaeoecological evidence on *Pinus cembra* (cf. Fig. 3 in main text)

Complementary information on palaeoecological methods

Pinus cembra-type pollen grains can be distinguished morphologically from *Pinus sylvestris*-type (including species from the subgenus *Pinus* or *Diploxylon*). However, many publications—especially older—do not differentiate between the two pollen types. In Europe, *Pinus peuce* also produces *Pinus* subgenus *Haploxylon*-type pollen like *P. cembra*, but the two species show clearly separated ranges and are unlikely to overlap in their postglacial occurrences.

The empirical limit is defined as the start of a closed curve in a pollen diagram, i.e., the presence of the same pollen type in consecutive samples and is conventionally interpreted as establishment of first local stands for wind-pollinated taxa (Birks & Tinner, 2016; Lang, 1994). Here, we defined the empirical limit as reached when *P. cembra* pollen was present in at least five consecutive samples that span at least 500 years.

References

Birks, H.J.B. & Tinner, W. (2016). European tree dynamics and invasions during the Quaternary. In Krumm, F., & Vítková, L. (Eds.), Introduced tree species in European forests: opportunities and challenges (pp. 22-43). Freiburg: European Forest Institute.

Lang, G. (1994) *Quartäre Vegetationsgeschichte Europas*, Jena: Gustav Fischer.

Table S3.1 Pollen records used for the compilation of palaeobotanical data of Swiss stone pine (*Pinus cembra*) presented in Fig. 3.

Site name	Country	Coordinates (WGS84)		Elevation [m asl.]	Empirical limit (cal. BP)[1]		References[2]
		Lat [°N]	Long [°E]		reached	older than	
Dortmunder Hütte	Austria	47.21091	11.00155	1915	9000		Heuberger (1977); Hüttemann & Bortenschlager (1987)
Egelsee	Austria	47.61312	12.17047	549	14200		Wahlmüller (1985)
Grosses Überling Schattseit-Moor	Austria	47.172222	13.9	1750	17000		Krisai et al. (1991)
Grünsee Reschenscheideck	Austria	46.862778	10.478056	1840	10700		Welten (1982b)
Katzenloch	Austria	47.341667	11.125	1220	10300		Wahlmüller (1985)
Kirchbichl	Austria	47.511111	12.090278	512		12500	Wahlmüller (1985)
Lake Jeserzersee	Austria	46.629167	14.03333	593	18200		Schmidt et al. (2012)
Längsee	Austria	46.7625	14.41944	548		19000	Huber et al. (2010)
Moosalmmoor	Austria	47.75	13.517	740	12800		Draxler (1977)
Schwarzsee Reschenscheideck	Austria	46.87	10.47833	1725		14700	Welten (1982b); van der Knaap & Ammann (1997)
Schwemm	Austria	47.66033	12.29357	664	16400		Oeggl (1988)
Seefelder See	Austria	47.3216	11.19205	1200	12600		Wahlmüller (1985)
Tauernmoos	Austria	47.16688	12.65191	2100		11700	Krisai (2006)
Čejčské jezero	Czech Republic	48.94215	16.96778	175		11900	Břízová (2009)
Čin-Čan-Tau	Czech Republic	50.518	15.203	265		14700	Svoboda et al. (2018)
Dářko	Czech Republic	49.64229	15.86933	622	13500		Roleček et al. (2020)
Hrabanovská černava	Czech Republic	50.21691	14.83009	184		16900	Petr & Novák (2014)
Plešné jezero	Czech Republic	48.776944	13.86258	1105		16000	Jankovská (2006); Pražáková et al. (2006)
Vlčí důl	Czech Republic	50.523	15.077	310		12100	Svoboda et al. (2018)
Canard	France	45.061489	5.931187	2055	4600		Ponel, de Beaulieu, & Tobolski (1992)
Cristol Lake	France	44.993611	6.5902778	2250	7300		Nakagawa (1998)
Lac des Boites	France	45.056	5.885	1560	5000		Nakagawa (1998)
Lac des Lauzons	France	44.782521	6.281765	2180	11600		Ponel et al. (2011)
Lac du Lait	France	45.314444	6.815556	2180	9000		Genries et al. (2009b)
Lac du Thyl	France	45.240556	6.499722	2038		8900	Genries et al. (2009a)
Lac Long Inférieur	France	44.057778	7.45	2114	10300		de Beaulieu (1977)
Lac Miroir	France	44.635278	6.793889	2210		4900	Nakagawa (1998)

Plateau de Prarion	France	45.884722	6.749444	1857	7700		de Beaulieu, Kostenzer, & Reich (1993)
Vallon de Provence	France	44.391111	6.404167	2075	6800		de Beaulieu (1977)
Kis-Mohos To	Hungary	48.4	20.4	310	16200		Willis et al. (1997)
Nagy-forrás	Hungary	47.8802222	20.0123056	685	14000		Pató et al. (2020)
Armentarga peat bog	Italy	46.04073389	9.87896194	2345		10400	Furlanetto et al. (2018)
Bondone	Italy	46.01896	11.0387	1550		13400	Grüger (1968)
Cerete Basso S3	Italy	45.8573889	9.990833	464		17000	Ravazzi et al. (2012)
Crotte Basse	Italy	45.76172	7.18191	2365		13000	Pini et al. (2017)
Dossaccio Bormio	Italy	46.47063	10.33554	1730		12800	Welten (1982b); van der Knaap & Ammann (1997)
Dura-Moor	Italy	46.63895	11.45624	2080		12500	Seiwald (1980)
Fersina	Italy	46.047222	11.118889	191		13900	Fuganti, Bazzoli, & Morteani (1998); Grüger & Morteani (2013)
Lago Basso	Italy	46.42272	9.29314	2250		12000	Wick & Tinner (1997)
Lago della Costa	Italy	45.269	11.739	7		20000	Kaltenrieder et al. (2009, 2010)
Lago di Annone	Italy	45.82128	9.351819	226		16500	Wick (1996)
Lago inferiore di Sangiatto	Italy	46.3193	8.287	1990		12000	van Vugt et al. (in prep.)
Lago Piccolo di Avigliana	Italy	45.05436	7.38985	356	15300		Finsinger & Tinner (2006); Finsinger et al. (2006, 2008, 2011); Vescovi et al. (2007); Lane et al. (2012)
Malschötscher Hotter	Italy	46.666111	11.458333	2050		10600	Seiwald (1980)
Palughetto	Italy	46.10237	12.40049	1040		15800	Vescovi et al. (2007)
Paùl 19-14	Italy	45.56	10.58	106		18000	Ravazzi et al. (2014)
Pian di Gembro	Italy	46.158	10.152	1350		19900	Pini (2002)
Rinderplatz	Italy	46.64569	11.48973	1780	13500		Seiwald (1980)
Schwarzsee	Italy	46.66644	11.43005	2033		11400	Seiwald (1980)
Sommersüss	Italy	46.76073	11.67907	870	15900		Seiwald (1980)
Tagliamento amphitheater (Lago di Ragogna)	Italy	46.177	13.002	188		20000	Monegato et al. (2007)
Torveraz	Italy	45.695278	6.860556	2415		9300	Miras et al. (2006); Millet et al. (2008)
Totenmoos	Italy	46.53	11.026	1718		16000	Heiss, Kofler, & Oeggl (2005)
Tourbière de Champlong	Italy	45.82638	7.64379	2320	9900		Brugiapaglia (1996)
Jasiel	Poland	49.3705	21.8875	680		13300	Szczepanek (1987)
Jasło	Poland	49.783333	21.46667	250		13800	Harmata (1995)
Puścizna Rękowiańska	Poland	49.47882	19.80199	656		11400	Obidowicz (1989, 1990, 1993)
Roztoki	Poland	49.74255	21.54422	230		14100	Harmata (1987)
Tarnawa Wyżna	Poland	49.11284	22.82548	670		14100	Ralska-Jasiewiczowa (1989)

Tarnowiec	Poland	49.73807	21.56259	220		13000	Harmata (1987)
Buhăiescu Mare	Romania	47.573611	23.64333	1918		11000	Geantă et al. (2014)
Gărgălău	Romania	47.573333	24.8025	1810	11000		Feurdean et al. (2016)
Iezerul Calimani	Romania	47.1125	25.273611	1650		20000	Farcas et al. (1999)
Lake Brazi (Tăul dintre Brazi)	Romania	45.396389	22.901667	1740		15700	Magyari et al. (2012)
Lake Bucura	Romania	45.3619167	22.87416667	2040		10200	Vincze et al. (2017)
Lake Galeş (Lacul Galeş)	Romania	45.385	22.90916667	2040		15200	Magyari et al. (2012)
Lake Lia	Romania	45.3520278	22.87758333	1910		17000	Vincze et al. (2017)
Pesteana	Romania	45.54396	22.80549	480		16600	Farcas & Tantau (2012)
Poiana Stiol	Romania	47.58333	24.8	1521	7300		Feurdean, Tanţău, & Fărcaş (2011)
Popradské pleso	Slovakia	49.15487	20.078	1513		9700	Carter et al. (2020)
Šafárka	Slovakia	48.882	20.575	600		20000	Kuneš et al. (2008)
Sivarna	Slovakia	49.313	20.663	610		14300	Kuneš et al. (2008)
Renče	Slovenia	45.89	13.66	60		20000	Monegato et al. (2015)
Aletschwald	Switzerland	46.389722	8.025556	2017		10000	Welten(1982a); van der Knaap & Ammann (1997)
Alpi di Robièi Val Bavona	Switzerland	46.445	8.518333	1936		12400	Welten (1982a); van der Knaap & Ammann (1997)
Bachalpsee	Switzerland	46.66944	8.020833	2265		12800	Lotter et al. (2006)
Balladrum	Switzerland	46.15919	8.74872	390		16400	Hofstetter et al. (2006)
Boehnigsee Goldmoos	Switzerland	46.259167	7.843056			10300	Markgraf (1969)
Burgaschisee	Switzerland	47.16969	7.66823	465	12200		Rey et al. (2017)
Gola di Lago	Switzerland	46.1044	8.965	985		13400	Höhn et al. (2022)
Gouillé Loéré	Switzerland	46.15006	7.35751	2503		11600	Tinner & Theurillat (2003)
Gouillé Rion	Switzerland	46.15726	7.36285	2343		11800	Tinner, Ammann, & Germann (1996)
Hinterburgsee	Switzerland	46.71801	8.06769	1519		12600	Heiri et al. (2003)
Hopschensee	Switzerland	46.2525	8.023056	2027	13000		Curdy et al. (2010)
Iffigsee	Switzerland	46.38679	7.40589	2065		11200	Schwörer, Henne, & Tinner (2014); Schwörer et al. (2014, 2015)
Il Fuorn	Switzerland	46.66286	10.20994	1805		8200	Stähli et al. (2006)
Lac d'Emines	Switzerland	46.32917	7.27588	2288		12000	Berthel, Schwörer, & Tinner (2012)
Lac de Bretaye	Switzerland	46.32603	7.07212	1780		11500	Thöle et al. (2016)
Lac de Champex	Switzerland	46.0283	7.1163	1467	12000		Rey et al. (2021)

Lac Superieur de Fully	Switzerland	46.176667	7.093611	2135		10900	Finsinger &Tinner (2007)
Lago di Origlio	Switzerland	46.05152	8.94329	416	16300		Tinner et al. (1999)
Lai Nair Schuls-Tarasp	Switzerland	46.776111	10.27778	1551	9000		Welten (1982b)
Las Gondas	Switzerland	46.902083	10.257277	2363		10400	Dietre et al. (2014)
Lauenensee	Switzerland	46.39684	7.33143	1381	13200		Rey et al. (2013)
Lej da Champfèr	Switzerland	46.46994	9.80624	1791		11800	Gobet et al. (2003, 2005); Henne et al. (2011)
Lej da San Murezzan	Switzerland	46.49394	9.84504	1768		11800	Gobet et al. (2003, 2005); Henne et al. (2011)
Lengi Egga	Switzerland	46.39429	7.97395	2557		12500	Tinner & Theurillat (2003)
Mont Carré Hérémence	Switzerland	46.153889	7.368611	2295		12700	Welten (1982a)
Oberaar	Switzerland	46.547222	8.25556	2380		11100	Ammann (1976, 1979)
Piano	Switzerland	46.320833	8.62	1439		11300	Valsecchi & Tinner (2010); Valsecchi et al. (2010)
Pillon Gsteig-Diablerets	Switzerland	46.359722	7.198611	1686	8200		Welten (1982a); van der Knaap & Ammann (1997)
Sägistalsee	Switzerland	46.6798	7.97638	1940		8900	Wick et al. (2003)
Simplon/Gampisch-Alter Spittel	Switzerland	46.23111	8.011389	1885		11600	Welten (1982a); van der Knaap & Ammann (1997)
Svityaz	Ukraine	51.505	23.838	157		13800	Schwörer et al. (2021)

[1] Empirical limit defined as at least 5 samples with presence in a row spanning at least 500 years, i.e. 5 samples AND 500 years

[2] See Appendix 3 for a full bibliography

Table S3.1 Macrofossil records used for the compilation of palaeobotanical data of Swiss stone pine (*Pinus cembra*) presented in Fig. 3.

Site name	Country	Coordinates (WGS84) Lat [°N]	Long [°E]	Elevation [m asl.]	First occurrence (cal. BP)[1] reached	older than	References
Kohltratten-Moor	Austria	47.043	14.421	1199	13600		Drescher-Schneider (2008)
Aigue Agnelle	France	44.73333333	6.883333333	2280	9200		Ali et al. (2005)
Lac des Grenouilles	France	44.09825	7.48358	1994	6600		Finsinger et al. (2021)
Lac du Lait	France	45.31444444	6.815555556	2180	9000		Genries et al. (2009b)
Lac du Loup	France	45.1875	6.537777778	2035	11300		Blarquez et al. (2010)
Lac du Thyl	France	45.24055556	6.499722222	2038	8500		Genries et al. (2009a)
Lake Miroir	France	44.634	6.792	2214		11400	Carcaillet & Blarquez (2017); Finsinger et al. (2019)
Queyras: Aigue Agnelle Valley	France	44.73333333	6.883333333	2200	6800		Talon (2010)
Saint-Michel-de Maurienne	France	45.25	6.5	1960	5900		Carcaillet (1998)
Tinée : Restefond	France	44.31666667	6.8	2650	3500		Talon (2010)
Ubaye: Upper Ubaye Valley	France	44.6	6.866666667	2430	6600		Talon (2010)
Nagy-forrás	Hungary	47.88022222	20.01230556	685	14600		Pató et al. (2020)
Fersina	Italy	46.047222	11.118889	191	12000		Fuganti, Bazzoli, & Morteani (1998); Grüger & Morteani (2013)
Lago Basso	Italy	46.42272	9.29314	2250	10300		Wick & Tinner (1997)
Lago di Colbricon Inferiore	Italy	46.28361111	11.76555556	1914	11000		Leys et al. (2014)
Lago di Ragogna	Italy	46.177	13.002	188	18000		Monegato et al. (2007)
Lago inferiore di Sangiatto	Italy	46.3193	8.287	1990	10500		van Vugt et al. (in prep.)
Lago Perso	Italy	44.90583333	6.797222222	2000	7000		Blarquez, Bremond, & Carcaillet (2010)
Tourbière de Champlong	Italy	45.82638	7.64379	2320	9000		Brugiapaglia (1996)
Lake Brazi (Tăul dintre Brazi)	Romania	45.39638889	22.90166667	1740	10000		Orbán et al. (2018)
Lake Lia	Romania	45.35202778	22.87758333	1910	11800		Orbán et al. (2018)
Preluca Tiganului	Romania	47.816	23.528	730	14100		Wohlfarth et al. (2001)
Popradské pleso	Slovakia	49.15487	20.078	1513	6300		Carter et al. (2020)
Sivarna	Slovakia	49.313	20.663	610		13200	Jankovska (1984)
Balladrum	Switzerland	46.15919	8.74872	390		16100	Hofstetter et al. (2006)
Feld Alp Holzmatten	Switzerland	46.659167	8.004167	2148		6300	Lotter et al. (2006)
Foppe	Switzerland	46.4575	8.79424	1470	14000		Vescovi et al. (2018)
Gola di Lago	Switzerland	46.1044	8.965	985	12600		Höhn et al. (2022)

Gouillé Loéré	Switzerland	46.15006	7.35751	2503	8900		Tinner & Theurillat (2003)
Gouillé Rion	Switzerland	46.15726	7.36285	2343	10700		Tinner, Ammann, & Germann (1996); Tinner & Kaltenrieder (2005); Kaltenrieder, Tinner, & Ammann (2005)
Hinterburgsee	Switzerland	46.71801	8.06769	1519	10800		Heiri et al. (2003)
Iffigsee	Switzerland	46.38679	7.40589	2065	7200		Schwörer, Henne, & Tinner (2014); Schwörer et al. (2014, 2015)
Lac de Bretaye	Switzerland	46.32603	7.07212	1780	10400		Thöle et al. (2016)
Lac de Fully	Switzerland	46.1788	7.09398	2135	8200		Finsinger & Tinner (2007)
Las Gondas	Switzerland	46.902083	10.257277	2363	10400		Dietre et al. (2014)
Las Gondas	Switzerland	46.902083	10.257277	2363		10400	Dietre et al. (2014)
Lej da Champfèr	Switzerland	46.46994	9.80624	1791	9300		Gobet et al. (2003, 2005); Henne et al. (2011)
Lej da San Murezzan	Switzerland	46.49394	9.84504	1768	10300		Gobet et al. (2003, 2005); Henne et al. (2011)
Sägistalsee	Switzerland	46.6798	7.97638	1940		9200	Wick et al. (2003)

[1] Indicating the age of first occurrence of *Pinus cembra* macrofossil in the record
[2] See reference list in Appendix 3 for a full bibliography

Pollen

Ammann, K. (1976). Der Oberaargletscher im 18., 19. und 20. Jahrhundert. *Zeitschrift für Gletscherkunde und Glazialgeologie*, XII, 253-291.

Ammann, K. (1979). Gletschernahe Vegetation in der Oberaar einst und jetzt - Historische Schwankungen des Oberaargletschers (Grimselpass, 2300 m, Schweiz) und ihr Einfluss auf die heutige Vegetation der Oberaar und einige Ergebnisse bisheriger Pollenanalysen Gletschernaher Profile. In Williams, O., & Tüxen, R. (Eds.), Werden and Vergehen von Pflanzengesellschaften (pp. 227-251). Vaduz: Cramer.

Berthel, N., Schwörer, C., & Tinner, W. (2012). Impact of Holocene climate changes on alpine and treeline vegetation at Sanetsch Pass, Bernese Alps, Switzerland. *Review of Palaeobotany and Palynology*, 174, 91-100.

Břízová, E. (2009). Quaternary environmental history of the Čejčské Lake (S. Moravia, Czech Republic). *Bulletin of Geosciences*, 84, 637-652.

Brugiapaglia, E. (1996). *Dynamique de la végétation tardiglaciaire et holocène dans les Alpes Italiennes nord-occidentales*. Unpublished MSc thesis, Marseille, France.

Carter, V.A., Bobek, P., Moravcová, A., Šolcová, A., Chiverrell, R.C., Clear, J.L., … Kuneš, P. (2020). The role of climate-fuel feedbacks on Holocene biomass burning in upper-montane Carpathian forests. Global and Planetary Change 193, 103264. https://doi.org/10.106/j.gloplacha.2020.103264

Curdy, P., Bullinger, J., Crotti, P., Valsecchi, V., & Tinner, W. (2010). Recherches archéologiques dans les régions du Simplon et de l'Albrun (Valais et Piémont) du Mésolitique a l'époque romaine. Pages 185-195 In S. Tzortzis, S., & Delestre, X. (Eds.) *Archéologie de la montagne européene* (pp. 185-195). Paris, France: Errance, Bibliothèque d'archéologie méditerranéene et africaine 4.

de Beaulieu, J.L. (1977). *Contribution pollenanalytique à l'histoire tardiglaciaire et Holocène de la végétation des Alpes méridionales françaices*. Doctoral dissertation. Université d'Aix-Marseille, Marseille, France.

de Beaulieu, J.L., Kostenzer, J., & Reich, K. (1993). Dynamique forestière holocène dans la haute vallée de l'Arve (Haute-Savoie) et migrations de *Abies* et *Picea* dans les Alpes occidentales. *Dissertationes Botanicae*, 196, 387-398.

Dietre, B., Walser, C., Lambers. K., Reitmaier, T. Hajdas, I., & Haas, J.N. (2014). Palaeoecological evidence for Mesolithic to Medieval climatic change and anthropogenic impact on the Alpine flora and vegetation of the Silvretta Massif (Switzerland/Austria). *Quaternary International*, 353, 3-16.

Draxler, I. (1977). Pollanalytische Untersuchungen von Mooren zur spät- und postglazialen Vegetationsgeschichte im Einzugsgebiet der Traun. *Jahrbuch der Geologischen Bundesanstalt*, 120, 131-163.

Farcas, S., de Beaulieu, J.-L., Reille, M., Coldea, G., Diaconeasa, B., Goeury, C., Goslar, T., & Jull, T. (1999). First ^{14}C dating of Late Glacial and Holocene pollen sequences from Romanian Carpathes. *Comptes Rendus de l'Académie des Sciences - Series III - Sciences de la Vie*, 322, 799-807.

Farcas, S., & Tantau, I. (2012). 16. Poiana Rusca Mountains (Romania): Pesteana peat bog. *Grana*, 51, 249-251.

Feurdean, A., Tanţău, I., & Fărcaş, S. (2011). Holocene variability in the range of distribution and abundance of *Pinus*, *Picea abies*, and *Quercus* in Romania; implications for their current status. *Quaternary Science Reviews*, 30, 3060-3075.

Feurdean, A., Gałka, M., Tanţău, I., Geantă, A., Hutchinson, S.M., & Hickler, T. (2016). Tree and timberline shifts in the northern Romanian Carpathians during the Holocene and the responses to environmental changes. *Quaternary Science Reviews*, 134, 100-113.

Finsinger, W., & Tinner, W. (2006). Holocene vegetation and land-use changes in response to climatic changes in the forelands of the southwestern Alps, Italy. *Journal of Quaternary Science*, 21, 243-258.

Finsinger, W., Tinner, W., van der Knaap, W.O, & Ammann, B. (2006). The expansion of hazel (*Corylus avellana* L.) in the southern Alps: a key for understanding its early Holocene history in Europe? *Quaternary Science Reviews*, 25, 612-631.

Finsinger, W., & Tinner, W. (2007). Pollen and plant macrofossils at Lac de Fully (2135 m a.s.l.): Holocene forest dynamics on a highland plateau in the Valais, Switzerland. *The Holocene*, 17, 1119-1127.

Finsinger, W., Belis, C., Blockley, S.P.E., Eicher, U., Leuenberger, M., Lotter, A.F., & Ammann, B. (2008). Temporal patterns in lacustrine stable isotopes as evidence for climate change during the late glacial in the Southern European Alps. *Journal of Paleolimnology*, 40, 885-895.

Finsinger, W., Lane, C.S., van den Brand, G.J., Wagner-Cremer, F., Blockley, S.P.E., & Lotter, A.F. (2011). The Lateglacial *Quercus* expansion in the southern European Alps: rapid vegetation response to a late Allerod climate warning? *Journal of Quaternary Science*, 26, 694-702.

Fuganti, A., Bazzoli, G., & Morteani, G. (1998). The Quaternary evolution of the Adige Valley near the city of Trento (Northern Italy) as deduced from wells and radiocarbon dating. Preliminary results. *Studi Trentini di Scienze Naturali. Acta Geologica*, 73, 93-97.

Furlanetto, G., Ravazzi, C., Pini, R., Vallè, F., Brunetti, M., Comolli, R., … Maggi, V. (2018). Holocene vegetation history and quantitative climate reconstructions in a high-elevation oceanic district of the Italian Alps. Evidence for a middle to late Holocene precipitation increase. *Quaternary Science Reviews*, 200, 212-236.

Geantă, A., Gałka, M., Tanţău, I., Hutchinson, S.M., Mîndrescu, M., & Feurdean, A. (2014). High mountain region of the Northern Romanian Carpathians responded sensitively to Holocene climate and land use changes: A multi-proxy analysis. *The Holocene*, 24, 944-956.

Genries, A., Mercier, L., Lavoie, M., Muller, S.D., Radakovitch, O., & Carcaillet, C. (2009a). The effect of fire frequency on local cembra pine populations. *Ecology*, 90, 476-486.

Genries, A., Muller, S.D., Mercier, L., Bircker, L., & Carcaillet, C. (2009b). Fires control spatial variability of subalpine vegetation dynamics during the Holocene in the Maurienne valley (French Alps). *Écoscience*, 16, 13-22.

Gobet, E., Tinner, W., Hochuli, P.A., van Leeuwen, J.F.N., & Ammann, B. (2003). Middle to Late Holocene vegetation history of the Upper Engadine (Swiss Alps): the role of man and fire. *Vegetation History and Archaeobotany*, 12, 143-163.

Gobet, E., Tinner, W., Bigler, C., Hochuli, P.A., & Ammann, B. (2005). Early-Holocene afforestation processes in the lower subalpine belt of the Central Swiss Alps as inferred from macrofossil and pollen records. *The Holocene*, 15, 672-686.

Grüger, J. (1968). Untersuchungen zur spätglazialen und frühpostglazialen Vegetationsentwicklung der Südalpen im Umkreis des Gardassees. *Botanische Jahrbücher für Systematik Pflanzengeschichte und Pflanzengeographie*, 88, 163-199.

Grüger, E., & Morteani, G. (2013). The pollen record of the 190 m core Fersina 2, an entirely Late-Glacial sediment sequence in the Adige valley at Trento (NE Italy). *Alpine Mediterranean Quaternary*, 26, 101-109.

Harmata, K. (1987). Late-Glacial and Holocene history of vegetation at Roztoki and Tarnowiec near Jasło (Jasło-Sanok Depression). *Acta Palaeobotanica*, 27, 43-65.

Harmata, K. (1995). A Late Glacial and Early Holocene profile from Jasło and a recapitulation of the studies on the vegetational history of the Jasło-Sanok Depression in the last 13 000 years. *Acta Palaeobotanica*, 35, 15-45.

Heiri, O., Wick, L., van Leeuwen, J.F.N., van der Knaap, W.O., & Lotter, A.F., (2003). Holocene tree immigration and the chironomid fauna of a small Swiss subalpine lake (Hinterburgsee, 1515 m asl). *Palaeogeography, Palaeoclimatology, Palaeoecology*, 189, 35-53.

Heiss, A.G., Kofler, W., & Oeggl, K. (2005). The Ulten Valley in South Tyrol, Italy: Vegetation and Settlement History of the Area, and Macrofossil Record from the Iron Age Cult Site of St. Walburg. *Palyno-Bulletin of the Institute of Botany, University of Innsbruck*, 1, 63-73.

Henne, P.D., Elkin, C.M., Reineking, B., Bugmann, H., & Tinner, W. (2011). Did soil development limit spruce (*Picea abies*) expansion in the Central Alps during the Holocene? Testing a palaeobotanical hypothesis with a dynamic landscape model. *Journal of Biogeography*, 38, 933-949.

Heuberger, H. (1977). Gletscher- und klimageschichtliche Untersuchungen im Zemmgrund. *Alpenvereins-Jahrbuch*, 102, 39-50.

Hofstetter, S., Tinner, W., Valsecchi, V., Carraro,, G., & Conedera, M. (2006). Lateglacial and Holocene vegetation history in the Insubrian Southern Alps - New indications from a small-scale site. *Vegetation History and Archaeobotany*, 15, 87-98.

Höhn, L., Leunda, M., Gobet, E., Tinner, W., & Schwörer, C. (2022). Vegetation response to rapid climate change during the Lateglacial – Early Holocene transition at Gola di Lago, southern Switzerland. *Boreas,* 51, 606-620

Huber, K., Weckström, K., Drescher-Schneider, R., Knoll, J., Schmidt, J., & Schmidt, R. (2010). Climate changes during the last glacial termination inferred from diatom-based temperatures and pollen in a sediment core from Längsee (Austria). *Journal of Paleolimnology*, 43, 131-147.

Hüttemann, H., & Bortenschlager, S. (1987). Beiträge zur Vegetationsgeschichte Tirols VI: Riesengebirge, Hohe Tatra - Zillertal, Kühtai. *Berichte des Naturwissenschaftlich-Medizinischen Vereins in Innsbruck*, 74, 81-112.

Jankovská, V. (2006). Late Glacial and Holocene history of Plešné Lake and its surrounding landscape based on pollen and palaeoalgological analyses. *Biologia, Bratislava* 61, S371-S385.

Kaltenrieder, P., Belis, C.A., Hofstetter, S., Ammann, B., Ravazzi, C., & Tinner, W. (2009). Environmental and climatic conditions at a potential glacial refugia site of tree species near the Southern Alpine glaciers. New insights from multiproxy sedimentary studies at Lago della Costa (Euganean Hills, Northeastern Italy). *Quaternary Science Reviews*, 28, 2647-2662.

Kaltenrieder, P., Procacci, G., Vannière, B., & Tinner, W. (2010). Vegetation and fire history of the Euganean Hills (Colli Euganei) as recorded by Lateglacial and Holocene sedimentary series from Lago della Costa (northeastern Italy). *The Holocene*, 20, 679-695.

Krisai, R., Burgstaller, B., Ehmer-Künkele, U., Schiffer, R., & Wurm, E. (1991). Die Moore des Ost-Lungaues - Heutige Vegetation, Enstehiung, Waldgeschichte ihrer Umgebung. *Sauteria*, 5, 1-240.

Krisai, R. (2006). Mooruntersuchungen im Stubachtal (Hohe Tauern, Salzburg). *Beitr. Naturk. Oberösterreichs*, 16, 105-147.

Kuneš, P., Pelánková, B., Chytrý, M., Jankovská, V., Pokorný, P., & Petr, L. (2008). Interpretation of the Last-Glacial Vegetation of Eastern-Central Europe Using Modern Analogues from Southern Siberia. *Journal of Biogeography*, 35, 2223–2236.

Lane, C.S., Blockley, S.P.E., Lotter, A.F., Finsinger, W., Filippi, M.L., & I.P. Matthews, I.P. (2012). A regional tephrostratigraphic framework for central and southern European climate archives during the Last Glacial to Interglacial transition: comparisons north and south of the Alps. *Quaternary Science Reviews*, 36, 50-58.

Lotter, A.F., Heiri, O., Hofmann, W., van der Knaap, W.O., van Leeuwen, J.F.N., Walker, I.R., & Wick, L. (2006). Holocene timber-line dynamics at Bachalpsee, a lake at 2265 m a.s.l. in the northern Swiss Alps. *Vegetation History and Archaeobotany*, 15, 295-307.

Magyari, E.K., G. Jakab, M. Bálint, Z. Kern, K. Buczkó, and M. Braun. 2012. Rapid vegetation response to Lateglacial and early Holocene climatic fluctuation in the South Carpathian Mountains (Romania). Quaternary Science Reviews 35: 116-130.

Markgraf, V. (1969). Moorkundliche und vegetations geschichtlichie untersuchungen an cinen Moorsee ander Waldgrenzeim Wallis. *Botanische Jahrbuecher*, 89, 1-63.

Millet, L., Ortu, E., Miras, Y., Heiri, O., Magny, M., & de Beaulieu, J.-L. (2008). Les assemblages de Chironomidae et les cortèges polliniques, outils de reconstitutions quantitatives des changements du climat holocène, une approche croisée au Col du Petit St Bernard, Lac 'Dessus- Verney', 2280 m. *Collection EDYTEM, Cahiers de Paléoenvironnement*, 6, 65-76.

Miras, Y., Millet, L., Guiter, F., Ponel, P., de Beaulieu, J.-L., & T. Goslar, T. (2006). Dynamique des écosystèmes et impact de l'homme dans le secteur du col du Petit Saint Bernard au cours de l'Holocène. *Actes du Programme Interreg "Alpis Graïa", 2-4 mars, 2006, Aoste, 31-50. Aosta, Italy*.

Monegato, G., Ravazzi, C., Donegana, M., Pini, R., Calderoni, G., & Wick, L. (2007). Evidence of a two-fold glacial advance during the last glacial maximum in the Tagliamento end moraine system (eastern Alps). *Quaternary Research*, 68, 284-302.

Monegato, G., Ravazzi, C., Culiberg, M., Pini, R., Bavec, M., Calderoni, G., Jež, J., & Perego, R. (2015). Sedimentary evolution and persistence of open forests between the south-eastern Alpine fringe and the Northern Dinarides during the Last Glacial Maximum. *Palaeogeography, Palaeoclimatology, Palaeoecology*, 436, 23-40.

Nakagawa, T. (1998). *Etudes palynologiques dans les Alpes Françaises centrales et méridionales: histoire de la végétation Tardiglaciaire et Holocène*. Doctoral dissertation. Université d'Aix-Marseille, Marseille, France.

Obidowicz, A. (1989). Type Region P-a: Inner West Carpathians- Nowy Targ Basin. *Acta Palaeobotanica*, 29, 11-15.

Obidowicz, A. (1990). Eine pollenanalytische und moorkundliche Studie zur Vegetationsgeschichte des Podhale-Gebietes (West-Karpaten). *Acta Palaeobotanica*, 30, 147-219.

Obidowicz, A. (1993). Wahania gornej granicy lasu w poznym plejstocenie i holocenie w Tatrach. In Kotarba, A. (editor) *Dokumentacja Geograficzna* (pp. 31-43).

Oeggl, K. (1988). Beiträge zur Vegetationgeschichte Tirols VII: Das Hochmoor Schwemm bei Wachsee. *Berichte des Naturwissenschaftlich-Medizinischen Vereins in Innsbruck*, 75, 37-60.

Pató, Z.A., Standovár, T., Gałka, M., Jakab, G., Molnár, M., Szmorad, F., & Magyari, E.K. (2020). Exposure matters: Forest dynamics reveal an early Holocene conifer refugium on a north facing slope in Central Europe. *The Holocene*, 30, 1833-1848.

Petr, L., & Novák, J. (2014). High vegetation and environmental diversity during the Late Glacial and Early Holocene on the example of lowlands in the Czech Republic. *Biologia*, 69, 847-862.

Pini, R. (2002). A high-resolution Late-Glacial – Holocene pollen diagram from Pian di Gembro (Central Alps, Northern Italy). *Vegetation History and Archaeobotany*, 11, 251-262.

Pini, R., Ravazzi, C., Raiteri, L., Guerreschi, A., Castellano, L., & Comolli, R. (2017). From pristine forests to high-altitude pastures: an ecological approach to prehistoric human impact on vegetation and landscapes in the western Italian Alps. *Journal of Ecology*, 105, 1580-1597.

Ponel, P., de Beaulieu J-L., & Tobolski, K. (1992). Holocene palaeoenvironments at the timberline in the Taillefer Massif, French Alps: A study of pollen, macrofossils and fossil insects. *The Holocene*, 2, 117-130.

Ponel, P., Court-Picon, M., Badura, M., Guiter, F., de Beaulieu, J.-L., Andrieu-Ponel, V., … Buttler, A. (2011). Holocene history of Lac des Lauzons (2180 m a.s.l.), reconstructed from multiproxy analyses of Coleoptera, plant macroremains and pollen (Hautes-Alpes, France). *The Holocene*, 21, 565-582.

Pražáková, M., Veselý, J., Fott, J., Majer, V., & Kopáček, J. (2006). The long-term succession of cladoceran fauna and palaeoclimate forcing: A 14,600-year record from Plešné Lake, the Bohemian Forest. *Biologia*, 61, S387–S399.

Ralska-Jasiewiczowa, M. (1989). Type region P-e: The Bieszczady Mountains. *Acta Palaeobotanica*, 29, 31-35.

Ravazzi, C., Badino, F., Marsetti, D., Patera, G., & P.J. Reimer, P.J. (2012). Glacial to paraglacial history and forest recovery in the Oglio glacier system (Italian Alps) between 26 and 15 ka cal BP. *Quaternary Science Reviews*, 58, 146-161.

Ravazzi, C., Pini, R., Badino, F., De Amicis, M., Londeix, L., & P.J. Reimer, P.J. (2014). The latest LGM culmination of the Garda Glacier (Italian Alps) and the onset of glacial termination. Age of glacial collapse and vegetation chronosequence. *Quaternary Science Reviews*, 105, 26-47.

Rey, F., Schwörer, C., Gobet, E., Colombaroli, D., van Leeuwen, J.F.N., Schleiss, S., & Tinner, W. (2013). Climatic and human impacts on mountain vegetation at Lauenensee (Bernese Alps, Switzerland) during the last 14,000 years. *The Holocene*, 23, 1415-1427.

Rey, F., Gobet, E., van Leeuwen, J.F.N., Gilli, A., van Raden, U.J., Hafner, A., … Tinner, W. (2017). Vegetational and agricultural dynamics at Burgäschisee (Swiss Plateau) recorded for 18,700 years by multi-proxy evidence from partly varved sediments. *Vegetation History and Archaeobotany*, 26, 571-586.

Rey, F., Brugger, S.O., Gobet, E., Andenmatten, R., Bonini, A., Inniger, H., … Schwörer, C. (2021). 14,500 years of vegetation and land use history in the upper continental montane zone at Lac de Champex (Valais, Switzerland). *Vegetation History and Archaeobotany*, https://doi.org/10.1007/s00334-021-00859-6

Roleček, J., Svitavská Svobodová, H., Jamrichová, E., Dudová, L., Hájková, P., Kletetschka, G., … Abraham, V. (2020). Conservation targets from the perspective of a palaeoecological reconstruction: the case study of Dářko peat bog in the Czech Republic. *Preslia*, 92, 87-114.

Schmidt, R., Weckström, K., Lauterbach, S., Tessadri, R., & Huber, K. (2012). North Atlantic climate impact on early late-glacial climate oscillations in the south-eastern Alps inferred from a multi-proxy lake sediment record. *Journal of Quaternary Science*, 27, 40-50.

Schwörer, C., Kaltenrieder, P., Glur, L., Berlinger, M., Elbert, J., Frei, S., … Tinner, W. (2014). Holocene climate, fire and vegetation dynamics at the treeline in the Northwestern Swiss Alps. *Vegetation History and Archaeobotany*, 23, 479-496.

Schwörer, C., Henne, P.D., & Tinner, W. (2014). A model-data comparison of Holocene timberline changes in the Swiss Alps reveals past and future drivers of mountain forest dynamics. *Global Change Biology*, 20, 1512-1526.

Schwörer, C., Colombaroli, D., Kaltenrieder, P., Rey, F., & Tinner, W. (2015). Early human impact (5000-3000 BC) affects mountain forest dynamics in the Alps. *Journal of Ecology*, 103, 281-295.

Schwörer, C., Gobet, E., van Leeuwen, J.F.N., Bögli, S., Imboden, R., van der Knaap, W.O., … Tinner, W. (2021). Holocene vegetation, fire and land use dynamics at Lake Svityaz, an agriculturally marginal site in northwestern Ukraine. *Vegetation History and Archaeobotany*, https://doi.org/10.1007/s00334-021-00844-z

Seiwald, A. (1980). Beiträge zur Vegetationsgeschichte Tirols IV: Natzer Plateau - Villanderer Alm. *Ber. nat.-med. Verein Innsbruck*, 67, 31-72.

Stähli, M., Finsinger, W., Tinner, W., & Allgöwer, B. (2006). Wildfire history and fire ecology of the Swiss National Park (Central Alps): new evidence from charcoal, pollen and plant macrofossils. *The Holocene*, 16, 805-817.

Svoboda, J., Pokorný, P., Horáček, I., Sázelová, S., Abraham, V., Divišová, M., … Perri, A. (2018). Late Glacial and Holocene Sequences in Rockshelters and Adjacent Wetlands of

Northern Bohemia, Czech Republic: Correlation of Environmental and Archaeological Records. *Quaternary International*, 465, 234–50

Szczepanek, K. (1987). Late-Glacial and Holocene pollen diagrams from Jasiel in the low Beshid Mountains, the Carpathians. *Acta Palaeobotanica*, 27, 9-26.

Szczepanek, K. (1989). Type region P-c: Low Beskidy Mountains. *Acta Palaeobotanica*, 29, 17-23.

Thöle, L., Schwörer, C., Colombaroli, D., Gobet, E., Kaltenrieder, P., van Leeuwen, J.F.N., & Tinner, W. (2016). Reconstruction of Holocene vegetation dynamics at Lac de Bretaye, a high-mountain lake in the Swiss Alps. *The Holocene*, 26, 380-396.

Tinner, W., Ammann, B., & Germann, P. (1996). Treeline fluctuations recorded for 12,500 years by soil profiles, pollen, and plant macrofossils in the Central Swiss Alps. *Arctic and Alpine Research*, 28, 131-147.

Tinner, W., Hubschmid, P., Wehrli, M., Ammann, B., & Conedera, M. (1999). Long-term forest fire ecology and dynamics in southern Switzerland. *Journal of Ecology*, 87, 273-289.

Tinner, W., & Theurillat, J.-P. (2003). Uppermost limit, extent, and fluctuations of the timberline and treeline ecocline in the Swiss Central Alps during the past 11,500 years. *Arctic, Antarctic, and Alpine Research*, 35, 158-169.

Valsecchi, V., & Tinner, W. (2010). Vegetation responses to climatic variability in the Swiss Southern Alps during the Misox event at the early–mid Holocene transition. *Journal of Quaternary Science*, 25, 1248-1258.

Valsecchi, V., Carraro, G., Conedera, M., & Tinner, W. (2010). Late-Holocene vegetation and land-use dynamics in the Southern Alps (Switzerland) as a basis for nature protection and forest management. *The Holocene*, 20, 483-495.

van Vugt, L., Garcés Pastor, S., Gobet, E., Brechbühl, S., Lammers, Y., Stengele, K., … Schwörer, C. (in prep.) A multiproxy study reveals climate and land use impacts on Holocene mountain vegetation of the Lepontine Alps, Italy.

van der Knaap, W.O., & Ammann, B. (1997). Depth-age relationships of 25 well-dated Swiss Holocene pollen sequences archived in the Alpine Palynological Data-Base. *Revue de Paléobiologie*, 16, 433-480.

Vescovi, E., Ravazzi, C., Arpenti, E., Finsinger, W., Pini, R., Valsecchi, V., … Tinner, W. (2007). Interactions between climate and vegetation during the Lateglacial period as recorded by lake and mire sediment archives in Northern Italy and Southern Switzerland. *Quaternary Science Reviews*, 26, 1650-1669.

Vincze, I., Orbán, I., Birks, H.H., Pál, I., Finsinger, W., Hubay, K., … Magyari, E.K. (2017). Holocene treeline and timberline changes in the South Carpathians (Romania): Climatic and anthropogenic drivers on the southern slopes of the Retezat Mountains. *The Holocene*, 27, 1613-1630.

Wahlmüller, N. (1985). Beiträge zur Vegetationsgeschichte Tirols V: Nordtiroler Kalkalpen. *Berichte des Naturwissenschaftlich-Medizinischen Vereins in Innsbruck*, 72, 101-144.

Welten, M. (1982a). *Vegetationsgeschichtliche Untersuchungen in den westlichen Schweizer Alpen: Bern-Wallis*. Denkschriften der Schweizerischen Naturforschenden Gesellschaft, Vol. 95.

Welten, M. (1982b). Pollenanalytische Untersuchungen zur Vegetationsgeschichte des Schweizerischen Nationalparks. *Ergebnisse der wissenschaftlichen Untersuchungen im Schweizerischen Nationalpark*, 16, 1-43.

Wick, L. (1996). Lateglacial and Early-Holocene palaeoenvironments in Brianza, N Italy. *Il Quaternario*, 9, 653-660.

Wick, L., & Tinner, W. (1997). Vegetation Changes and Timberline Fluctuations in the Central Alps as Indicators of Holocene Climatic Oscillations. *Arctic and Alpine Research*, 29, 445-458.

Wick, L., van Leeuwen, J.F.N., van der Knaap, W.O., & Lotter, A.F. (2003). Holocene vegetation development in the catchment of Sägistalsee (1935 m asl), a small lake in the Swiss Alps. *Journal of Paleolimnology*, 30, 261–272.

Willis K.J., Braun, M., Sümegi, P., & Tòth, A. (1997). Does soil change cause vegetation change or vice versa? A temporal perspective from Hungary. *Ecology*, 78, 740-750.

Macrofossils

Ali, A.A., Carcaillet, C., Talon, B., Roiron, P., & Terral, J.-F. (2005). *Pinus cembra* L. (arolla pine), a common tree in the inner French Alps since the early Holocene and above the present tree line: a synthesis based on charcoal data from soils and travertines. *Journal of Biogeography*, 32, 1659-1669.

Blarquez, O., Bremond, L., & Carcaillet, C. (2010). Holocene fires and a herb-dominated understorey track wetter climates in subalpine forests. *Journal of Ecology*, 98, 1358-1368.

Blarquez, O., Carcaillet, C., Bremond, L., Mourier, B., & Radakovitch, O. (2010). Trees in the subalpine belt since 11 700 cal. BP: origin, expansion and alteration of the modern forest. *The Holocene*, 20, 139-146.

Brugiapaglia, E. (1996). *Dynamique de la végétation tardiglaciaire et holocène dans les Alpes Italiennes nord-occidentales*. Unpublished MSc thesis, Marseille, France.

Carcaillet, C. (1998). A spatially precise study of Holocene fire history, climate and human impact within the Maurienne valley, North French Alps. *Journal of Ecology*, 86, 384-396.

Carcaillet, C., & Blarquez, O. (2017). Fire ecology of a tree glacial refugium on a nunatak with a view on Alpine glaciers. *New Phytologist*, 216, 281-290

Carter, V.A., Bobek, P., Moravcová, A., Šolcová, A., Chiverrell, R.C., Clear, J.L., … Kuneš, P. (2020). The role of climate-fuel feedbacks on Holocene biomass burning in upper-montane Carpathian forests. Global and Planetary Change 193, 103264. https://doi.org/10.106/j.gloplacha.2020.103264

Dietre, B., Walser, C., Lambers. K., Reitmaier, T. Hajdas, I., & Haas, J.N. (2014). Palaeoecological evidence for Mesolithic to Medieval climatic change and anthropogenic impact on the Alpine flora and vegetation of the Silvretta Massif (Switzerland/Austria). *Quaternary International*, 353, 3-16.

Drescher-Schneider, R. (2008). Das Kohltratten-Moor südlich von Schloss Lind. Neue pollen- und grossrestanalytische Ergebnisse zur spät- und postglazialen Vegetations- und Klimaentwicklung im Gebiet Neumarkt (Steiermarkt Österreich). *Mitteilungen Naturwisssenschaftlicher Vererein für Steiermark*, 137, 63-84.

Finsinger, W., & Tinner, W. (2007). Pollen and plant macrofossils at Lac de Fully (2135 m a.s.l.): Holocene forest dynamics on a highland plateau in the Valais, Switzerland. *The Holocene*, 17, 1119-1127.

Finsinger, W., Schwörer, C., Heiri, O., Morales-Molino, C., Ribolini, A., Giesecke, T., … Tinner, W. (2019). Fire on Ice and Frozen Trees? Inappropriate Radiocarbon Dating Leads to Unrealistic Reconstructions. *New Phytologist*, 222, 657–662

Finsinger, W., Vanel, Q., Ribolini, A., & Tinner, W. (2021). Early-to-late-Holocene vegetation and fire dynamics at the treeline in the Maritime Alps. *Vegetation History and Archaeobotany*, 30, 507-524.

Fuganti, A., Bazzoli, G., & Morteani, G. (1998). The Quaternary evolution of the Adige Valley near the city of Trento (Northern Italy) as deduced from wells and radiocarbon dating. Preliminary results. *Studi Trentini di Scienze Naturali. Acta Geologica*, 73, 93-97.

Genries, A., Mercier, L., Lavoie, M., Muller, S.D., Radakovitch, O., & Carcaillet, C. (2009a). The effect of fire frequency on local cembra pine populations. *Ecology*, 90, 476-486.

Genries, A., Muller, S.D., Mercier, L., Bircker, L., & Carcaillet, C. (2009b). Fires control spatial variability of subalpine vegetation dynamics during the Holocene in the Maurienne valley (French Alps). *Écoscience*, 16, 13-22.

Gobet, E., Tinner, W., Hochuli, P.A., van Leeuwen, J.F.N., & Ammann, B. (2003). Middle to Late Holocene vegetation history of the Upper Engadine (Swiss Alps): the role of man and fire. *Vegetation History and Archaeobotany*, 12, 143-163.

Gobet, E., Tinner, W., Bigler, C., Hochuli, P.A., & Ammann, B. (2005). Early-Holocene afforestation processes in the lower subalpine belt of the Central Swiss Alps as inferred from macrofossil and pollen records. *The Holocene*, 15, 672-686.

Grüger, E., & Morteani, G. (2013). The pollen record of the 190 m core Fersina 2, an entirely Late-Glacial sediment sequence in the Adige valley at Trento (NE Italy). *Alpine Mediterranean Quaternary*, 26, 101-109.

Heiri, O., Wick, L., van Leeuwen, J.F.N., van der Knaap, W.O., & Lotter, A.F., (2003). Holocene tree immigration and the chironomid fauna of a small Swiss subalpine lake (Hinterburgsee, 1515 m asl). *Palaeogeography, Palaeoclimatology, Palaeoecology*, 189, 35-53.

Henne, P.D., Elkin, C.M., Reineking, B., Bugmann, H., & Tinner, W. (2011). Did soil development limit spruce (*Picea abies*) expansion in the Central Alps during the Holocene? Testing a palaeobotanical hypothesis with a dynamic landscape model. *Journal of Biogeography*, 38, 933-949.

Hofstetter, S., Tinner, W., Valsecchi, V., Carraro,, G., & Conedera, M. (2006). Lateglacial and Holocene vegetation history in the Insubrian Southern Alps - New indications from a small-scale site. *Vegetation History and Archaeobotany*, 15, 87-98.

Höhn, L., Leunda, M., Gobet, E., Tinner, W., & Schwörer, C. (2022). Vegetation response to rapid climate change during the Lateglacial – Early Holocene transition at Gola di Lago, southern Switzerland. *Boreas*, 51, 606-620.

Jankovska, V. (1984). Late Glacial finds of *Pinus cembra* in the Lubovnianska kotlina basin. *Folia Geobotanica et Phytotaxonomica*, 19, 323-325

Kaltenrieder, P., Tinner, W., & Ammann, B. (2005). Zur Langzeitökologie des Lärchen-Arvengürtels in densüdlichen Walliser Alpen. *Botanica Helvetica*, 115, 137-154.

Leys, B., Carcaillet, C., Blarquez, O., Lami, A., Musazzi, S., & Trevisan, R. (2014). Resistance of mixed subalpine forest to fire frequency changes: the ecological function of dwarf pine (*Pinus mugo* ssp. *mugo*). *Quaternary Science Reviews*, 90, 60-68.

Lotter, A.F., Heiri, O., Hofmann, W., van der Knaap, W.O., van Leeuwen, J.F.N., Walker, I.R., & Wick, L. (2006). Holocene timber-line dynamics at Bachalpsee, a lake at 2265 m a.s.l. in the northern Swiss Alps. *Vegetation History and Archaeobotany*, 15, 295-307.

Monegato, G., Ravazzi, C., Donegana, M., Pini, R., Calderoni, G., & Wick, L. (2007). Evidence of a two-fold glacial advance during the last glacial maximum in the Tagliamento end moraine system (eastern Alps). *Quaternary Research*, 68, 284-302.

Orbán, I., Birks, H.H., Vincze, I., Finsinger, W., Pál, I., Marinova, E., … Magyari, E.K. (2018). Treeline and timberline dynamics on the northern and southern slopes of the Retezat Mountains (Romania) during the late glacial and the Holocene. *Quaternary International*, 477, 59-78.

Pató, Z.A., Standovár, T., Gałka, M., Jakab, G., Molnár, M., Szmorad, F., & Magyari, E.K. (2020). Exposure matters: Forest dynamics reveal an early Holocene conifer refugium on a north facing slope in Central Europe. *The Holocene*, 30, 1833-1848.

Schwörer, C., Kaltenrieder, P., Glur, L., Berlinger, M., Elbert, J., Frei, S., … Tinner, W. (2014). Holocene climate, fire and vegetation dynamics at the treeline in the Northwestern Swiss Alps. *Vegetation History and Archaeobotany*, 23, 479-496.

Schwörer, C., Henne, P.D., & Tinner, W. (2014). A model-data comparison of Holocene timberline changes in the Swiss Alps reveals past and future drivers of mountain forest dynamics. *Global Change Biology*, 20, 1512-1526.

Schwörer, C., Colombaroli, D., Kaltenrieder, P., Rey, F., & Tinner, W. (2015). Early human impact (5000-3000 BC) affects mountain forest dynamics in the Alps. *Journal of Ecology*, 103, 281-295.

Talon, B. (2010). Reconstruction of Holocene high-altitude vegetation cover in the French southern Alps: evidence from soil charcoal. *The Holocene*, 20, 35-44.

Thöle, L., Schwörer, C., Colombaroli, D., Gobet, E., Kaltenrieder, P., van Leeuwen, J.F.N., & Tinner, W. (2016). Reconstruction of Holocene vegetation dynamics at Lac de Bretaye, a high-mountain lake in the Swiss Alps. *The Holocene*, 26, 380-396.

Tinner, W., & Theurillat, J.-P. (2003). Uppermost limit, extent, and fluctuations of the timberline and treeline ecocline in the Swiss Central Alps during the past 11,500 years. *Arctic, Antarctic, and Alpine Research*, 35, 158-169.

Tinner, W., & Kaltenrieder, P. (2005). Rapid responses of high-mountain vegetation to early Holocene environmental changes in the Swiss Alps. *Journal of Ecology*, 93, 936-947.

van Vugt, L., Garcés Pastor, S., Gobet, E., Brechbühl, S., Lammers, Y., Stengele, K., … Schwörer, C. (in prep.) A multiproxy study reveals climate and land use impacts on Holocene mountain vegetation of the Lepontine Alps, Italy.

Vescovi, E., Tinner, W., Beer, R., van Leeuwen, J.F.N., Steinhauser, U., Ziegler, S.,… Carraro, G. (2018). Vegetation History of the Upper Leventina Valley from Roman to Neolithic

Times, recorded by pollen, spores, macrofossils and charcoal. *Zurich Studies in Archaeology*, 12, 207-225.

Wick, L., & Tinner, W. (1997). Vegetation Changes and Timberline Fluctuations in the Central Alps as Indicators of Holocene Climatic Oscillations. *Arctic and Alpine Research*, 29, 445-458.

Wick, L., van Leeuwen, J.F.N., van der Knaap, W.O., & Lotter, A.F. (2003). Holocene vegetation development in the catchment of Sägistalsee (1935 m asl), a small lake in the Swiss Alps. *Journal of Paleolimnology*, 30, 261–272.

Wohlfarth, B., Hannon, G., Feurdean, A., Ghergari, L., Onac, B.P, & Possnert, G. (2001). Reconstruction of climatic and environmental changes in NW Romania during the early part of the last deglaciation (∼ 15,000—13,600 cal yr BP). *Quaternary Science Reviews*, 20, 1897-1914.